

Report Number CCEER-94-3

**SUMMARY OF PRETEST ANALYSIS OF
CAZENOVIA CREEK BRIDGE**

Bruce M. Douglas
Emmanuel M. Maragakis
Shiping Feng

Prepared for

**National Center for Earthquake Engineering Research
National Science Foundation
New York Department of transportation**

by

**The Center for Civil Engineering Earthquake Research
Department of Civil Engineering
University of Nevada
Reno, Nevada 89557**

April 1994

ABSTRACT

As part of a study to evaluate the basic dynamic characteristics of the southbound bridge of Cazenovia Creek, a detailed parametric study was carried out and is described in this report.

A 3-dimensional analysis model was developed for the modal analysis of the bridge. Also a simple model was constructed for the analysis of the bridge. For the evaluation of the influence of the soil stiffness at the foundation, 8 soil stiffnesses were employed in the modal analyses for both the 3-D and the 2-D models. Finally, for considering the effect of the actual state of the bridge, two further modifications were made in the 3-dimensional model.

The transverse frequencies of the 3-D model and the 2-D model were compared and the difference in frequencies of two models were less than 10 percent for all the comparisons. The influence of the soil stiffness on the dynamic behavior of the bridge should be considered when the soil stiffnesses are less than 10 times the standard value. In the pretest parameter study, the frequencies of both the cracked and uncracked structure were calculated. The properties in the cracked structure had more influence on the fundamental frequency than the other frequencies.

Three loading cases were performed in the parameter study. In the first loading case, two concentrated loads of 150 kips each were horizontally applied to the $1/3$ points of the bridge. In the second case, 150 kips were applied to one $1/3$ point of the bridge. In the third case, a load of 150 kips was applied to the abutment. The participation factors, displacement and acceleration time histories corresponding to these three loading cases are discussed in the report.

Acknowledgements

The study presented in this report was part of a project which has been mainly funded the Federal Highway Administration and the National Center for Earthquake Engineering Research. The financial support of all the funding agencies is particularly acknowledged.

Mr. Ayae Malik of the New York Department of Transportation is thanked for providing valuable information and comments about the construction drawings of the bridges over the Cazenovia Creek.

SUMMARY OF PRETEST ANALYSIS OF CAZENOVIA CREEK BRIDGE

CONTENTS

Abstract	i
Acknowledgements	iii
List of Tables.	vi
List of Figure.	vi
Chapter 1 Introduction.	1
1.1 Background	1
1.2 Objective.	2
Chapter 2 Bridge Description	3
2.1 General	3
2.2 Description	3
Chapter 3 3-Dimensional Analysis Model.	6
3.1 General.	6
3.2 Simplifying Assumptions.	6
3.3 Elements in 3-D Model.	7
3.4 Mass Distribution of 3-D Model.	10
Chapter 4 Simple 2-Dimensional Analysis Model.	11
4.1 General.	11
4.2 Simplifying Assumptions.	11

4.3 Elements in 2-D Model.	12
4.4 Mass Distribution of 2-D Model.	13
Chapter 5 Model Analysis.	14
5.1 General.	14
5.2 Frequencies of 3-D Model and Simple Model.	14
5.3 Evaluation of Foundation Stiffness	15
Chapter 6 Parameter Study of Quick-Released Excitation	17
6.1 General.	17
6.2 Mode Analysis of Simple Testing Model	18
6.3 Pretest Results and Observation	19
6.4 Modification of 3-D Model	22
Chapter 7 Summary and Conclusions	27
7.1 Summary	27
7.2 Conclusions	32

LIST OF TABLES

- Table 3.1 Element Cross-Sectional Properties
- Table 5.1 Transverse Frequencies for Southbound Lane
- Table 6.1 Frequencies of Simple Model of Southbound Lane
- Table 6.2 Participation Factors of Simple Model
- Table 6.3 Frequencies for Modified 3-D Model

LIST OF FIGURES

- Figure 2.1 South Bound Lanes of Cazenvoia Creek Overpass
- Figure 2.2 Deck Section of South Bound Lane
- Figure 2.3 Pier Bent Elevation of South Bound Lane
- Figure 3.1 3-Dimensional Model of South Bound Lane
- Figure 4.1 2-Dimensional Simple Model of South Bound Lane
- Figure 4.2 Pier Model for Equivalent Spring Stiffness
- Figure 5.1 Soil Stiffness vs. Fundamental Frequencies
- Figure 5.2 Soil Stiffness vs. Second Frequencies
- Figure 6.1 Load Cases for Pretest of Simple Model
- Figure 6.2 The First Transverse Mode Shape of Simple Model
- Figure 6.3 The Second Transverse Mode Shape of Simple Model
- Figure 6.4 The Third Transverse Mode Shape of Simple Model
- Figure 6.5 The Fourth Transverse Mode Shape of Simple Model
- Figure 6.6 Displacement at Joint 1 in Load Case 1
- Figure 6.7 Displacement at Joint 6 in Load Case 1
- Figure 6.8 Displacement at Joint 11 in Load Case 1

Figure 6.9 Acceleration at Joint 1 in Load Case 1

Figure 6.10 Acceleration at Joint 6 in Load Case 1

Figure 6.11 Acceleration at Joint 11 in Load Case 1

Figure 6.12 Displacement at Joint 1 in Load Case 2

Figure 6.13 Displacement at Joint 6 in Load Case 2

Figure 6.14 Displacement at Joint 11 in Load Case 2

Figure 6.15 Acceleration at Joint 1 in Load Case 2

Figure 6.16 Acceleration at Joint 6 in Load Case 2

Figure 6.17 Acceleration at Joint 11 in Load Case 2

Figure 6.18 Acceleration at Joint 6 (Mode 1) in Load Case 2

Figure 6.19 Acceleration at Joint 6 (Mode 2) in Load Case 2

Figure 6.20 Acceleration at Joint 6 (Mode 4) in Load Case 2

Figure 6.21 Displacement at Joint 1 in Load Case 3

Figure 6.22 Displacement at Joint 6 in Load Case 3

Figure 6.23 Displacement at Joint 11 in Load Case 3

Figure 6.24 Acceleration at Joint 1 in Load Case 3

Figure 6.25 Acceleration at Joint 6 in Load Case 3

Figure 6.26 Acceleration at Joint 11 in Load Case 3

Figure 6.27 Acceleration at Joint 6 (Mode 1) in Load Case 3

Figure 6.28 Acceleration at Joint 6 (Mode 2) in Load Case 3

Figure 6.29 Frame-type Model for Deck and Girder at Pier

Figure 6.30 Frame-type Model for Deck and Girder at Abutment

Figure 6.31 Deflection of Frame-Type Model at Pier

Figure 6.32 Deflection of Frame-Type Model at Abutment

Figure 6.33 First Transverse Mode Shape of Modified 3-D Model

Figure 6.34 Second Transverse Mode Shape of Modified 3-D Model

Figure 6.35 Third Transverse Mode Shape of Modified 3-D Model

Figure 6.36 Fourth Transverse Mode Shape of Modified 3-D Model

Figure 6.37 First Vertical Mode Shape of Modified 3-D Model

Figure 6.38 First Longitudinal Mode Shape of Modified 3-D Model

CHAPTER 1. INTRODUCTION

1.1 Background

The studies in the seismic vulnerability of existing highway bridges have added significant new knowledge to seismic retrofit technologies for the national highways. However, the present guidelines for seismic retrofit of highway bridges are 10-15 years old, and recent experience has given new insight into bridge and highway response during earthquake.

A range of studies is therefore being carried out which consists of vulnerability assessment, retrofit technologies, and criteria and guideline development.

As a part of this research project, field testing is planned for two, three span continuous bridges over the Cazenovia Creek in Western New York. Both the Albany and regional offices of the New York Department of Transportation are planning to replace existing steel bearings with elastomeric conventional bearings on one bridge and seismic isolation bearings on the other. Large displacement, quick-release testing is proposed as the means of activating relative movement between the superstructure and substructure. Resulting insights regarding in situ pier stiffness and bearing

behavior are anticipated to lead to useful conclusions about seismic displacement demands and the relative performance of the various old and new bearing types.

1.2 Objective

To evaluate the basic dynamic characteristics of the South Bound Lanes of the Cazenovia Creek Overpass, a detailed parametric study was carried out and is described in this report. A 3-dimensional model was developed for the modal analysis of the bridge, and a simple model was also developed for this study.

The frequencies of the bridge based on the 3-dimensional as well as the simple models were calculated and compared each other. In the calculation, the foundation stiffnesses effected the bridge frequencies for both the 3-dimensional and the simple analysis models. Time history analyses, simulating the quick-released loading were also performed. Three loading cases were considered in the analysis. For considering the effect of the actual state of the bridge, two further modifications were made in the 3-dimensional model.

CHAPTER 2 BRIDGE DESCRIPTION

2.1 General

The Cazenovia Creek Overpass, shown in Figure 2.1, is located at the Aurora Expressway in the New York state. Built in 1967, the Overpass consists of two independent parallel bridges. One is for the South Bound Lanes and the other for the North Bound Lanes. The two bridges are three span reinforced concrete structures and have same kind of the pier bent supports and the seat-type abutments, however, the southbound bridge is longer and wider than the northbound. In this report, all the pretest studies are concentrated on the southbound bridge.

2.2 Description

The southbound bridge is a three span continuous structure with an overall length of 200.90 feet and a height of 34 feet. The bridge elevation is higher at the north abutment than at the south abutment. The average vertical grade is 0.98 percent.

The deck section is composed of a 7.5 inch thick by 48.25 foot wide reinforced concrete deck slab and seven W36X150 steel girders. The seven steel girders are laterally supported by channel beams in the transverse direction at the pier bents and the

abutments. Typical cross-section of the deck is shown in Figure 2.2. The north and south end spans are 59.68 feet and 55.26 feet long, respectively, while the middle span is 86 feet long.

Two pier bents support the superstructure. The pier bent elevation is illustrated in Figure 2.3. The pier bent consists of a tapered cap-beam and two reverse-tapered columns. The beam is deeper at the pier column connections.

Expansion bearings are located at the north and the south abutments and the south pier. The bridge superstructure supported on these three bearings can freely move in longitudinal direction but are restrained in the transverse and vertical directions. The bearing joints are designed to freely rotate about the transverse and vertical axes of the bridge, but can't rotate about the longitudinal axis of the bridge.

A fixed bearing hinge is located at the top of the north pier bent. The bearing joint is restrained in all the translation directions and the rotations except for a rotation about the global transverse axis of the bridge.

The seat-type abutments consist of a concrete seat and a concrete backwall. The horizontal section of the abutment is a L shape. The concrete seat is 8 foot wide and 4 foot deep. The backwall is 18 inch wide and an average 8 foot high.

Steel pile foundations support the two intermediate pier bents as well as the two abutments. The pier bent foundation of the bridge consists of a rectangular concrete pile cap and 14 10BP42 steel bearing piles. The abutment foundation consists of concrete pile cap and 22 10BP42 Steel pile. The foundation soil consists of nine layers. Seven of layers are below the pile cap, one of layer is around the pile cap, and the last one is above the pile cap. For a detailed description of the pile footing and surrounding soil see Ref. 1.

CHAPTER 3. 3-DIMENSIONAL ANALYSIS MODEL

3.1 General

A 3-Dimensional analysis model of the southbound bridge was developed (Figure 3.1). The 3-D modal consisted of 56 nodes, 57 linear beam elements, 4 linear truss elements and 6 linear ground spring elements. The analyses were performed using the SAP-90 program. This chapter describes the geometric configuration of the model and the element properties of the model.

3.2 Simplifying Assumptions

In implementing the 3-Dimensional computer model, certain considerations were made concerning the southbound bridge:

(1) The Cazenovia Creek Overpass has a superelevation of 3.24 percent to accommodate high-speed traffic and a vertical grade of approximately 0.98 percent in the longitudinal direction, both of them were considered in the model.

(2) The pier bents and the abutments of the bridge have a skew angle of 9.70 degrees, the skew was considered in the model.

(3) In the calculation of the cross sectional properties, no concrete reinforcement was considered.

3.3 Elements in 3-D Model

The southbound bridge model was composed of several element types as follows:

(1) The beam elements were used for the bridge deck. Since the deck section was composed of the concrete slab and the steel girder, the composite cross-sectional properties were calculated based on a concrete compression strength of 5000 psi and A36 steel. No reinforcement was used in the determination of the cross sectional properties. Table 3.1 shows the sectional properties.

(2) The cap-beam in the pier bent was modelled with eight beam elements, and each column in the bent was modelled with two beam elements. The section properties at both the ends of the elements were calculated. A linear variation of the properties along the element length was specified. The sectional properties used in the model are listed in Table 3.1.

3) Because of the difference in the elevation between the deck section center of mass and the pier cap-beam center of mass, it was necessary to use rigid beam elements to connect the deck element to the cap-beam elements. Two vertical rigid elements were used at the

top of each pier bent. One connected the deck element to the bearing hinge and the other connected the bearing hinge to the center of the cap-beam of the pier. A joint between these two elements was located at the bearing connection on the each pier (This will be explained later). A rigid element was also used to model the very-stiff upper joint region for the each pier column. Section properties for these rigid elements were empirically chosen to ensure rigidity and are listed in Table 3.1.

4) To avoid local bending effects at the connection of the cap-beam to the vertical rigid element, two diagonal rigid elements were used to connect the deck elements to the cap-beam elements at the each pier. These two elements can only carry axial force and are truss elements.

5) One beam element was used to model the concrete footing (pile cap) of the each pier bent. Sectional properties for this element are list in Table 3.1.

6) A beam element was also used to model the L shaped concrete wall at the each abutment. A rigid element was used to take into account the difference in elevation between the deck section center of mass and the bearing location at the top of each abutment. Cross sectional properties of the elements for the abutments are also listed in Table 3.1.

7) Foundations of the piers and the abutments were modelled using the spring elements of 'SAP90'. Three stiffness components of each spring element were used at the foundations of piers and the abutments. Two of these components were in the longitudinal and transverse directions of the bridge, and the third one was the rotation about transverse axis of the bridge. The vertical displacement, rotation about the longitudinal axis of the bridge and torsion at the foundations were ignored. Fixed boundary conditions were used for these spring components. The initial ground spring stiffnesses in the model were estimated based on past experience and they are listed in Table 3.1. These initial ground spring stiffnesses were referred to the 'standard soil stiffness' in this report and they were changed in the different study cases (see Chapter 5).

8) Special rigid elements were used between the bridge deck and the bearing hinge at the abutments and the south pier bent. The elements were fixed at the two ends to carry bending moment about a local axis parallel to the longitudinal direction of the bridge. On the other hand, the elements were released about the other local axis which paralleled the transverse direction of the bridge so that the deck may freely move in the longitudinal direction. A zero torsion stiffness was input for the bearing joint to allow free rotation about the vertical axis of the bridge. The cross sectional properties in the model were shown in Table 3.1.

9) A rigid element was used between the deck and the bearing joint at the north pier bent. The cross sectional properties of the element were chosen to ensure the rigidity. However, at the bearing joint, the bending inertia about the transverse axis of the bridge was assumed to be zero to ensure the free rotation of the bearing hinge.

3.4 Mass Distribution of 3-D Model

Lumped mass distribution was used in the 3-D model. The masses were concentrated at the model nodes translation directions. The masses associated with rotational degree of freedom were assumed to be zero.

CHAPTER 4. 2-DIMENSIONAL SIMPLE ANALYSIS MODEL

4.1 General

A 2-Dimensional simple model of the southbound bridge was developed as shown in Figure 4.1. The simple model was only used for transverse analyses of the bridge.

4.2 Simplify Assumptions

In developing the simple model, the following assumptions were made:

(1) The simple model allows the longitudinal and transverse displacements only. Since no vertical displacements of the bridge were involved in the dynamic analysis of the 2-D model, all the node masses of the vertical direction of the bridge were assumed to be zero in this simple model.

(2) The north abutment was restrained in the longitudinal direction so that no significant longitudinal movement of the bridge was involved in the simple model analysis. However, because of axial deformation of the deck members, slight displacements of the nodes along the longitudinal direction of the bridge occur in

the analysis.

(3) All other assumptions were same as those used in developing the 3-D model.

4.3 Elements in 2-D Model

The 2-D simple model of the southbound bridge was composed three types of the elements:

(1) Beam elements were used to model the composite bridge deck. The cross sectional properties were same as the 3-D model and listed in Table 3.1.

(2) A equivalent spring element was used for the each pier bent. To determine the equivalent spring stiffness of the pier bent, a static horizontal unit load was applied to the top of pier model (Figure 4.2) in the transverse direction of the bridge. The inverse value of the difference between the top displacement of the pier bent and the footing displacement was defined as equivalent pier stiffness. The cross sectional properties of the pier members and the foundation spring stiffness in the pier model were same as the 3-D model of the bridge. It should also be noted that the skew angle of pier bent was considered in the calculation.

A horizontal unit load also was applied to the top of the

abutment in order to determine an equivalent spring stiffness for the abutment and soil. The inverse value of the top displacement of the abutment was defined as the equivalent spring stiffness at the abutment. In the calculation, the abutment properties and the foundation spring stiffness were same as the 3-D model. And the skew of the abutment was considered in the abutment model.

(3) The ground spring element was used at the pier foundation. One end of the spring connected to the ground and the other end connected to the pier footing mass. The spring stiffness was same as that used in the 3-D model of the bridge.

4.4 Mass Distribution 2-D Model

Lumped mass distribution was used in the 2-D model. The masses were concentrated at the model nodes at which the translational displacements were defined. The mass associated with the rotational degree of freedom was taken to be zero.

CHAPTER 5. MODEL ANALYSIS

5.1 General

The model analysis results of the 3-D model and the 2-D simple model are described in this chapter. The transverse frequencies of two models were compared. For the evaluation of the effect of the soil stiffness on the foundation, 8 soil stiffnesses, increasing in magnitude, were employed in the analyses of both the 3-D and the 2-D models.

5.2 Frequencies of 3-D Model and Simple Model

Comparison of the transverse frequencies for the South Bound Bridge are shown in Table 5.1. The transverse frequencies of the 3-D model were generally larger than those of the simple model except for the cases in which the lower soil stiffnesses of 0.2 or 0.5 times the standard soil stiffness were used. The difference of frequencies between the 3-D and the 2-D simple models were less than 10 percent for all the comparisons. Smaller frequency differences in the higher modes can be seen in the low soil stiffness cases. The blank cells in the table are high transverse frequencies which can't be easily associated with the mode shape.

5.3 Evaluation of foundation stiffness.

The spring stiffness for the simulation of the soil property at the bridge foundation was an unknown parameter. To evaluate the influence of the soil spring stiffness on the dynamic characteristics of the structure model, eight cases of the soil spring stiffness were assumed and the corresponding dynamic analyses of the 3-D model were performed. The standard soil spring stiffness was estimated based on experience. In the other analysis cases, 1/5, 1/2, two, five, ten, twenty and 1000 times as much as the standard soil stiffness were employed.

Figure 5.1 shows the relationship between the soil spring stiffness and the fundamental frequencies. The fundamental frequencies greatly changed while the soil spring stiffness varied from the 0.2 to five times the standard value. The frequencies, however, changed only slightly when 10 times or higher the standard soil stiffness were used. Note that the non-scaled last soil stiffness in the figure was 1000 times the standard value. The curves from the 3-D model had similar shape with the simple model.

The second frequencies increased rapidly while the soil stiffnesses were in the low value region (Figure 5.2). The frequencies increased slowly when the soil stiffnesses were larger than 10 times the standard value. Based on the above observations, the effect of the soil stiffness on the dynamic behavior of the

southbound bridge should be considered in the region of less than 10 times the standard soil stiffness.

CHAPTER 6. PARAMETER STUDY OF QUICK-RELEASED TESTING

6.1 General

A pretest parameter study was carried out for the quick-release testing of the southbound bridge.

The 2-D simple model of the bridge was employed for three loading cases. The cracked section properties of 2-D model were considered in the cases studied. In the calculation, the cross-sectional properties of 85 percent uncracked composite deck and 70 percent uncracked concrete pier bents were used. Note that the 85 percent sectional properties of the composite deck was determined by combining the properties of 70 percent uncracked concrete deck slab and using 100 percent of the steel girders. A soil spring stiffness of 5 times the standard value was used for the testing simple model.

Three loading cases were performed in the parameter study. In the first loading case, two concentrated loads, 150 kips each, were applied to nodes 7 and 15 at the top of the pier bents. In the second case, a single load of 150 kips was applied to the top of the north pier. In the third case, a load of 150 kips was applied to the top of the north abutment. The loading cases are shown in

Fig. 6.1.

Because the SAP 90 can't directly simulate the free vibration of the structure due to a quick-release static loading, the following procedure was used in the pretest study: 1) A constant time history loading was applied to the desired location of the bridge to produce a forced vibration; 2) When time history responses of the bridge approached a constant state, a zero dynamic load replacing the previous constant load was applied to the structure; 3) From this, the constant response of the bridge due to the constant time history loading was considered to be the initial condition of the quick-released test and the response due to the zero load is the free vibration after the quick-released static load.

6.2 Mode Analysis of Simple Model

A modal analysis was performed determine the frequencies of the 2-D simple model for the pretest study. The first four transverse frequencies of the simple model with the cracked sectional properties are shown in Table 6.1. Also shown in this table are the uncracked simple model frequencies. The frequencies of the cracked structure were 5 percent lower than the uncracked structure. The properties in the cracked structure had more influence on the fundamental frequency than the other frequencies.

The first four transverse mode shapes of the 2-D simple model with cracked structural properties are shown in Figures 6.2 - 6.5. The first mode shape was symmetric about the midpoint in the longitudinal direction of the bridge. The largest and the smallest values were the midpoint of the bridge and the abutments of the bridge, respectively. The second mode shape had large values at both the abutments and a zero at the location near the midpoint of the bridge. Mode shape 3 had smaller values at the pier bents and larger values at the abutments. The fourth mode shape had its largest values at the pier bents, a zero near the midpoint of the bridge and the smaller values at both the abutments.

6.3 Pretest Results and Observations

As the previously mentioned, the three loading cases were performed for the pretest analyses of the southbound bridge of the Cazenovia Creek Overpass. Because the cracked structural properties may be more consistent with the current state of the bridge, the three loading cases were applied to the cracked simple bridge model.

The participation factors of the cracked simple model in the different loading cases are shown in the Table 6.2. The participation factors were determined by the following formula:

where, $V(0)$ - initial displacements of the model due to the loads

$$y_j = \frac{(\phi_j)^T [M] (V(0))}{(\phi_j)^T [M] (\phi_j)}$$

where, $V(0)$ - initial displacements of the model due to the loads corresponding to the cases studied,

(ϕ_j) - the j th mode shape,

$[M]$ - the structural mass matrix.

In the first loading case, two of 150 kips were transversely applied to joint 7 and 15 which were almost symmetric about the model midpoint. Therefore, the participation factor (Table 6.2) of the first mode was dominant and the other three participation factors were less than 2 percent of the first mode.

The displacements of joints 1, 6 and 11 in the first loading case are shown in Figures 6.6, 6.7 and 6.8, respectively. Joints 1, 6 and 11 were located at the north abutment, the 1/4 point and the midpoint, respectively. The loads were quick released at the 6th second in the figures. The displacements of joints 1, 6 and 11 were 0.00487 in., 0.0462 in. and 0.0636 in. at the moment of load released. From the figures, no responses from the higher frequencies were presented since the first mode participation factor was much larger than the other modes. The acceleration responses of joints 1, 6 and 11 are illustrated in Figures 6.9, 6.10 and 6.11, respectively. The maximum accelerations at joints 1, 6 and 11 were 0.033g, 0.21g and 0.25g, respectively.

In the second loading case, a single 150 kips load was applied

to the top of the north pier of the bridge. The participation factor of the first mode shape was still dominant but the second mode participation factor was about 14 percent of the first mode factor (Table 6.2).

The displacements of joints 1, 6 and 11 in the second loading case are shown in Figures 6.12, 6.13 and 6.14. The displacements of joints 1, 6 and 11 were 0.00414 in., 0.0284 in. and 0.0325 in. at the time the load was quick released. From the figures, no responses from the higher frequencies were obvious since the first mode participation was larger than the other modes (Table 6.2). And also the second frequency was approximate 2 times the first frequency so that a slight influence of the second mode can be seen in the peak response of the displacement time history. The acceleration responses of joints 1, 6 and 11 are illustrated in Figures 6.15, 6.16 and 6.17, respectively. The maximum acceleration of 0.088g at joint 1 was 2.67 times as much as the response in load case 1. The maximum acceleration at joints 6 was 0.152g which was larger than the maximum acceleration of 0.130g at joint 11 since the load was only applied at the north pier bent. The acceleration corresponding to the higher frequencies can be seen from the responses at joints 1 and 6. The acceleration components corresponding to the transverse mode shapes 1, 2 and 4 at joint 6 are show in Figures 6.18, 6.19 and 6.20. The third acceleration component was too small to show at the same scale as the 1, 2 and 4 components.

The displacements of joints 1, 6 and 11 in the third loading case are shown in Figures 6.21, 6.22 and 6.23. The loads were quick released at the 6th second in the figure. At the moment of load release, the displacements at joints 1, 6 and 11 were 0.00853 in., 0.00483 in. and 0.00201 in.. From the figures, the responses corresponding to the higher frequencies are significant in the displacements at joints 1 and 6 because the second and the third mode participation factors were larger than the first mode in this loading case (Table 6.2). The acceleration responses of joints 1, 6 and 11 are illustrated in Figures 6.24, 6.25 and 6.26, respectively. The maximum acceleration of 0.130g at joint 1 was 3.94 times and 1.48 times as much as load case 1 and 2, respectively. Since the load was only applied to the abutment the maximum acceleration at joints 6 was 0.106g which was less than the maximum acceleration of 0.130g at joint 1. Both the accelerations at joints 1 and 6 were larger than the maximum acceleration at joint 11 since the effect of the first mode shape was less than the 2nd and the 3rd. The acceleration components corresponding to the 3rd transverse mode shapes 1 and 2 at joint 6 are show in Figures 6.27 and 6.28. The acceleration component of the second mode was larger than the first mode.

6.4 Modification of 3-D Model

To consider the effect of the actual state of the bridge, two further modifications were made in the 3-Dimensional model.

The first modification of 3-D model was to use hinges instead of the rollers between the deck girder and the abutment because the joints at the top of the abutments may be restrained in the longitudinal direction.

The second modification was based on the possibility of deflection of the deck steel girders in the transverse direction of the bridge. The seven girders of the southbound bridge set on the pier bents and the abutments and they were connected to each other by the channel beams in the transverse direction (Figure 2.2). To evaluate the transverse deflection between the deck slab and the bottom of the steel girder, frame-type models were developed for the cross sections at the piers as well as at the abutments as shown in Figures 6.29 and 6.30, respectively. The top horizontal members in the model represented the deck slab. The effective width of the deck slab of 1.83 feet was determined by using the provisions of ACI code. The middle horizontal members in the model represented the connecting beams between the steel girders.

For the model at the piers (Figure 6.29), there were five vertical members at the each steel girder location. The middle three of these members were used to model the rigidity of connection zone of the steel girders to the connecting beam and a large stiffness was used for these members. The top and bottom members were used for the unconnected parts of the girders. For the model at the abutment (Figure 6.30), there were three vertical

members at each girder location. The first two were used to represent the rigid connection zone. The third one at the bottom was used for the unconnected parts of the girder. Sectional properties of the vertical members were determined based on the dimensions of the steel girder and stiffeners.

A unit static load was applied to the top of frame-type model and the deflections of the frame are shown in Figure 6.31 and 6.32. Based on the top deflection of the steel girder in the transverse direction of the bridge, the rigid truss members at the pier top and the rigid beam member at the abutment top in the 3-Dimensional model were modified.

The effective area of the truss members connecting the deck elements to the pier elements (Figure 3.1) was determined by:

$$\Delta = \sum \frac{N^2 L}{EA}$$

where, Δ - top deflection of truss.

N - force of truss member due to unit load.

A - effective area of truss member.

The effective area was used to replace the stiffness of the original rigid truss members in the 3-D model.

A effective moment of inertia of the beam element connecting

the deck element to the abutment element was determined by:

$$\Delta = \frac{L^3}{3EI}$$

where, Δ - top deflection of element

I - effective moment of inertia of beam element.

The effective moment of inertia was used to replace the stiffness of the rigid beam element at the abutment in the original 3-D model.

The first four transverse frequencies of the modified 3-D model are shown in Table 6.3. Three soil stiffness conditions were considered in these recalculations. The transverse frequencies were generally smaller than the original model due to the decreased stiffness between the deck and piers as well as deck and abutments.

The first longitudinal and vertical frequencies were shown in the first two columns of Table 6.3. Because hinges instead of the rollers at the top of the abutments were used in the modified 3-D model, the longitudinal frequencies were much larger than the original model. The first vertical frequencies of the modified 3-D model differed only slightly from the original model since the foregoing modification of the model has little to do with vertical properties of the bridge.

The first four transverse mode shapes of the bridge are shown in Figure 6.33-6.36. Note that 0.75 times the standard soil stiffness was used for this calculation. Because of the very soft soil conditions, the large transverse deflections at the pier bents and the abutment bases can be observed in the all mode shapes except for the fourth transverse mode shape at pier bases. The relative transverse deflections between the deck and the steel girder bottom can be seen in the figures. The relative transverse deflections at the abutments were larger than those at the piers because the abutment stiffness was very large and the frame-type model at the abutment had a smaller stiffness than at the pier bent.

The first vertical and longitudinal mode shapes of the modified 3-D model are shown Figures 6.37 and 6.38, respectively. Because of the roller existing between the deck and the pier in the longitudinal direction of the bridge, the south pier didn't carry any longitudinal force even through there were the displacement and the rotation at the top of the south pier. Because the rigid connection of the deck to the abutment rotated, a vertical displacement at the deck can be observed in the longitudinal mode shape.

Chapter 7 SUMMARY AND CONCLUSIONS

7.1 Summary

As part of a study to evaluate the basic dynamic characteristics and the earthquake response of the southbound bridge of Cazenovia Creek, a detailed parametric study was carried out and is described in this report. A 3-dimensional analysis model was developed for the modal analysis of the bridge, and a simple model was established for the modal analysis, the time history and the pretest parameter studies.

The southbound bridge is a three span reinforced concrete structures with an overall length of 200.90 feet and a height of 34 feet. The bridge elevation is higher at the north abutment than at the south abutment. Three spans are 59.68 feet, 86 feet and 55.26 feet long from the north to the south, respectively.

The deck section consists of a reinforced concrete deck slab and seven W36X150 steel girders. The seven steel girders are lateral supported by the channel beams in the transverse direction at the pier bents and the abutments. Two pier bents support the superstructure. The pier bent consists of a tapered cap-beam and two reverse-tapered columns.

The expansion bearings are located at the top of the two abutments and the south pier. The bridge superstructure supported on these three bearings is designed to move freely in the longitudinal direction of the bridge but is restrained in the transverse and vertical directions. The bearing joints can freely rotate about the transverse and vertical axes of the bridge but not rotate about the longitudinal axis of the bridge. A fixed bearing hinge is located at the top of the north pier bent. The bearing joint is restrained in all the translation directions and the rotations except for a rotation about the global transverse axis of the bridge.

The seat-type abutments consist of a concrete seat and a concrete backwall. The abutment foundation consists of a concrete pile cap and 22 10BP42 Steel pile. The pier bent foundation of the bridge consists of a rectangular concrete pile cap and 14 10BP42 steel bearing piles. The foundation soil consists of nine layers.

A 3-Dimensional mathematical model of the South Bound Lane was developed for the SAP90 analyses. The 3-D model consists of 56 nodes, 57 linear beam elements, 4 linear truss elements and 6 linear ground spring elements.

Beam elements were used for the superstructure consisting of the concrete slab and the steel girders. The cap-beam in the each bent was modelled with eight beam elements and each column in the

bent was modelled with two beam elements.

Because of the difference in the elevation between the deck section center of gravity and the pier cap-beam center of gravity, two vertical rigid elements were used at the top of each pier bent. One connected the deck element to the bearing hinge and the other connected the bearing hinge to the center of the cap-beam of the pier. Rigid elements between the bridge deck and the bearing hinge at the abutments and the south pier carry the bending moment about the global longitudinal axis of the bridge, but allow the deck freely moving in this direction. The rigid element between the deck and the bearing joint at the north pier bent restrained all the translations and rotations except for a rotation about the global transverse axis of the bridge. A rigid element was also used to model the very-stiff upper joint region for the each pier column.

To avoid the local bending effects at the connection of the cap-beam connection to the rigid element, two diagonal rigid truss elements were used to connect the deck elements to the cap-beam elements at the each pier.

One beam element was used to model the concrete wall at the each abutment. One rigid element was used to consider the difference in elevation between the deck section center of gravity and the bearing location at the top of each abutment.

The Foundations of the piers and the abutments were modelled by 'SAP90' spring elements. Three stiffness components of each spring element were used at the foundation of the piers and the abutments. Two of these components were along the longitudinal and the transverse directions of the bridge and the third one was rotation about the transverse axis of the bridge. The vertical displacement, rotation about the longitudinal axis of the bridge and torsion at the foundations were ignored and represented by the fixed boundary conditions.

The lumped mass distribution was concentrated at the model nodes at which the translational displacements are defined. The masses associated with rotational degree of freedom were assumed to be zero.

A 2-Dimensional simple model of the bridge was also established for both the modal and time history analysis of the bridge. The simple model was only used for the transverse analysis the bridge.

The 2-D simple model of the South Bound Lane was composed beam elements and spring elements. Beam elements were used to model the composite bridge deck. The cross sectional properties were same as the 3-D model. Equivalent spring elements were used for the pier bents and the abutments. In the calculation of the equivalent spring stiffness, the cross sectional properties of the pier

members were same as the 3-D model of the bridge. The ground spring element was also used at the pier foundation. One end of the spring connected to the ground and the other end connected to the pier footing mass. The soil spring stiffness was same as the 3-D model of the bridge.

Lumped masses along the translation direction were concentrated at the nodes and the masses associated with rotational degree of freedom were assumed to be zero.

For the evaluation of the influence of the soil stiffness at the foundation, 8 soil stiffnesses were employed in the modal analyses for both the 3-D and the 2-D models.

Using the 2-D simple model of the bridge, a pretest parameter study was carried out for the quick-released testing of the South Bound Lane of the Creek Cazenovia Overpass. In the calculation, the cross-sectional properties of 85 percent of the uncracked composite deck and 70 percent uncracked concrete piers were used. A soil spring stiffness of 5 times the standard value was used for the pretest analysis using simple model.

Three loading cases were performed in the parameter study. In the first loading case, two concentrated loads of 150 kips each were applied to the 1/3 points of the bridge. In the second case, 150 kips was applied to one 1/3 point of the bridge. In the third

case, a load of 150 kips was applied to the abutment.

For considering the effect of the actual state of the bridge, two further modifications were made in the 3-dimensional model.

The first modification of 3-D model was to use hinges instead of the rollers between the deck girder and the abutment because the joints at the top of the abutments may actually be restrained in the longitudinal direction.

The second modification was based on including the deflection of the deck steel girders in the transverse direction of the bridge. To evaluate the relative deflection between the deck slab and the bottom of the steel girder, frame-type models were developed for the pier bent and abutment sections. A unit static load was applied to the top of the frame-type model and the deflections of the frame were calculated. Based on the top deflection of the steel girder in the transverse direction of the bridge, the rigid truss members at the pier top and the rigid beam member at the abutment top of the 3-Dimension model were modified. The sectional properties of these members were recalculated using standard the structural mechanics principles. The new values were used in the modified 3-D analysis model.

7.2 CONCLUSIONS

1. The transverse frequencies of the 3-D model were generally larger than those of the simple model except for the cases in which the smaller soil stiffness of 0.2 or 0.5 times standard soil stiffness were used. The difference in frequencies between the 3-D and the 2-D simple models were less than 10 percent for all the comparisons. The smaller soil stiffnesses caused smaller frequency differences in the higher modes.

2. The fundamental frequencies greatly changed when the soil spring stiffness varied from the 0.2 to five times as much as the standard value. The frequencies, however, changed only slightly when soil stiffnesses 10 times or higher the original soil stiffness were used. The second frequencies increased rapidly when the soil stiffnesses were in the low value region. The frequencies increased slowly when the soil stiffness became larger than 10 times the standard soil stiffness. Based on the observations, the influence of the soil stiffness on the dynamic behavior of the bridge should be considered when the soil stiffnesses are less than 10 times the standard soil stiffness.

3. The frequencies of the cracked structure were 5 percent lower than the uncracked structure. The properties in the cracked structure had more influence on the fundamental frequency than the other frequencies.

4. Two 150 kips loads in the first quick release loading case

were symmetrically applied to the bridge model. Therefore, the participation factor of mode 1 was dominant and the other three participation factors were less than 2 percent of the factor of mode 1.

5. The displacements caused by the first loading showed no influence from the higher frequencies, because the first mode participation factor was much larger than the other modes.

6. Even though a single 150 kips load in the second loading case was applied to the north pier of the bridge, the participation factor of the first mode shape was still dominant and the second participation factor was about 14 percent the first mode factor. The displacements contributions from the higher frequencies were not present in a significant way. However, the accelerations corresponding to the higher frequencies could be seen from the responses at the abutments and the at 1/4 point. The maximum acceleration at the loaded node was larger than the other node accelerations. The maximum acceleration at the abutment was 2.67 times as much as the abutment response in load case 1.

7. In the third loading case, the displacement responses corresponding to the higher frequencies were significantly present in the displacements at the abutment and at the 1/4 point because the second and the third mode participation factors were larger than the first mode. The maximum acceleration at the abutment was

larger than loading case 1 and 2. However, the maximum acceleration at the 1/4 point was less than abutment response since the load was only applied at joint 1. The effect of the first mode was less than the 2nd and the third mode, therefore, the accelerations at the midpoint of the bridge were less than at the 1/4 point and the abutments.

8. After considering the relative deflection between the deck and the pier bent, the first four transverse frequencies of the modified 3-D model were generally smaller than the original model due to the decreased stiffness between the deck and piers as well as deck and abutments.

9. After considering the fixity at the abutment supports, the longitudinal frequencies of the bridge became much larger than the original model.

10. The first vertical frequencies of the modified 3-D model had differed only slightly from the original model since the modification of the model had little to do with the vertical behavior of the bridge.

11. Because of the very soft soil conditions used in the modified model, large transverse deflections at the pier and the abutment bases were observed in the all mode shapes except for the

fourth transverse mode shape at the pier bases. The relative transverse deflections between the deck and the steel girder bottom can be seen from the results. The relative transverse deflections at the abutments were larger than those at the piers because of the larger abutment stiffness and the smaller frame-type model stiffness.

12. The first vertical and the longitudinal mode shapes of the modified 3-D model showed that the south pier didn't carry any longitudinal force because of the rollers between the deck and the pier in the longitudinal direction of the bridge. Because the rigid connection of the deck to the abutment rotated in the longitudinal mode shape, a vertical deflection of the deck was displayed.

Table 3.1 Element Cross-Sectional Properties

Member type	Cross-Sectional Area (ft ²)	Bending Inertia about Weak-Axis (ft ⁴)	Bending Inertia about Strong-Axis (ft ⁴)	Torsional Inertia (ft ⁴)
Deck	45.62	65.29	9136.2	3.922
Cap-Beam 1 (11,19,35,43)	9.50	7.94	40000.*	12.82
Cap-Beam 2 (12,18,36,42)	14.25	26.79	40000.*	26.63
Cap-Beam 3 (13,17,37,41)	19.00	63.50	40000.*	40.65
Cap-Beam 4 (14,16,38,40)	17.12	46.49	40000.*	35.10
Cap-Beam 5 (15,39)	15.25	32.83	40000.*	29.57
Column 1 (20,21,44,45)	14.25	10.69	26.79	26.63
Column 2 (22,23,46,47)	15.75	11.81	36.18	31.04
Column 3 (24,25,48,49)	17.25	12.94	47.53	35.47
Truss Element	10000*	-	-	-
Rigid Element	1000*	10000*	10000*	10000*
Abutment	115.5	857.	1298.7	83.45
Footing	52.5	109.4	482.3	311.4

Numbers in () are nodes of the elements;
 * Value chosen to ensure adequate rigidity.

Table 5.1 Transverse Frequencies for South Bound Lane

Soil Stiffness	Model	f_1	f_2	f_3	f_4
1/5 * Soil Stiffness	3-D	2.90	3.14	7.68	26.00
	Simple	3.08	3.18	8.30	25.12
1/2 * Soil Stiffness	3-D	4.41	4.91	8.72	26.07
	Simple	4.50	4.93	9.15	25.20
1 * Soil Stiffness	3-D	5.82	6.88	10.02	26.19
	Simple	5.61	6.83	10.12	25.33
2 * Soil Stiffness	3-D	7.16	9.59	12.10	-
	Simple	6.70	9.47	12.03	25.87
5 * Soil Stiffness	3-D	8.23	14.60	17.13	24.15
	Simple	7.53	14.18	16.80	25.99
10 * Soil Stiffness	3-D	8.59	18.93	23.29	28.67
	Simple	7.83	18.20	22.37	28.03
20 * Soil Stiffness	3-D	8.77	21.89	31.97	35.37
	Simple	8.02	20.74	29.62	34.94
1000 * Soil Stiff.	3-D	8.99	23.76	-	-
	Simple	8.22	22.54	55.55	68.94

Soil Spring Stiffness:

$$K_{lat.} = 43,200 \text{ kips/ft}$$

$$K_{rot.} = 1.17 \times 10^5 \text{ kips.ft/rad}$$

Table 6.1 Frequencies of Simple Model of South Bound Lane
(5 * Soil Stiffness)

	f_1	f_2	f_3	f_4
Uncracked Sections	7.53	14.18	16.80	25.99
Cracked Sections	6.79	13.97	16.61	24.24

Cracked Section: $I_{deck} = 0.85 I_{gross}$
 $I_{pier} = 0.70 I_{gross}$

Table 6.2 Participation Factors of Simple Model (South)

Loading Case	mode 1	mode 2	mode 3	mode 4
1	0.02654	-0.000166	-0.000479	0.0000637
2	0.01363	0.001895	-0.000301	-0.001030
3	0.001562	0.002384	0.00213	0.000610

$$Y_j = \frac{(\phi_j)^T [M] (v(0))}{(\phi_j)^T [M] (\phi_j)}$$

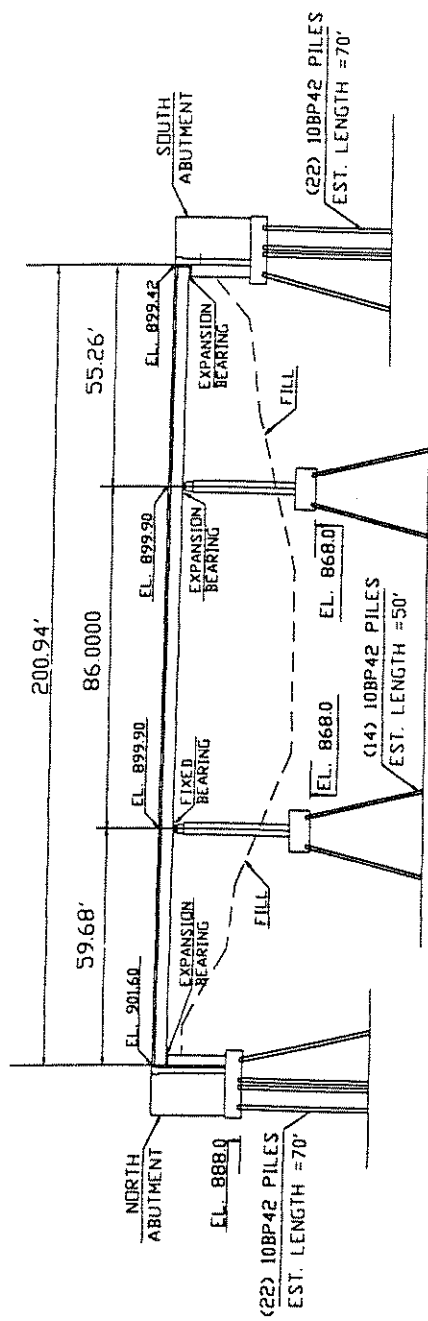
Table 6.3 Frequencies for Modified 3-D Model
(Cracked, Girder Deflection)

Soil Stiffness	First Vert.	First Long.	f ₁ (Trans)	f ₂ (Trans)	f ₃ (Trans)	f ₄ (Trans)
1/2*S.S.	4.024	4.11	4.28	4.84	7.73	23.80
3/4*S.S.	4.023	4.18	4.82	5.83	8.44	22.63
1*S.S.	4.024	4.20	5.28	6.64	9.25	23.28

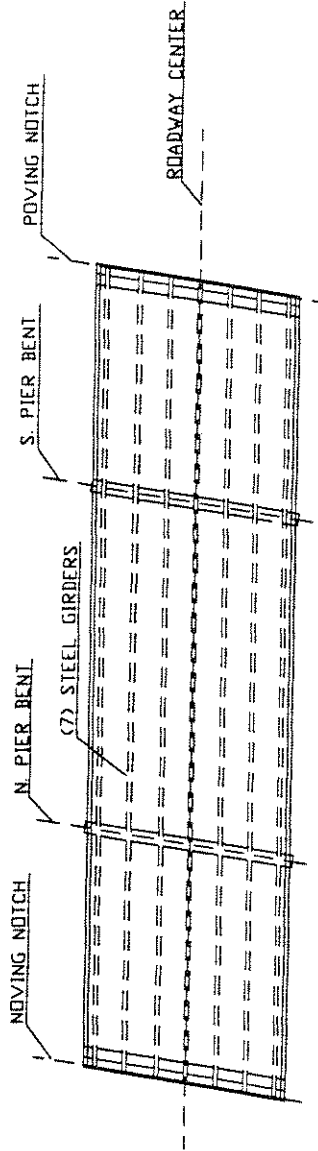
S.S. -- Soil Spring Stiffness:

$$K_{lat.} = 43,200 \text{ kips/ft}$$

$$K_{rot.} = 1.17 \times 10^5 \text{ kips.ft/rad}$$

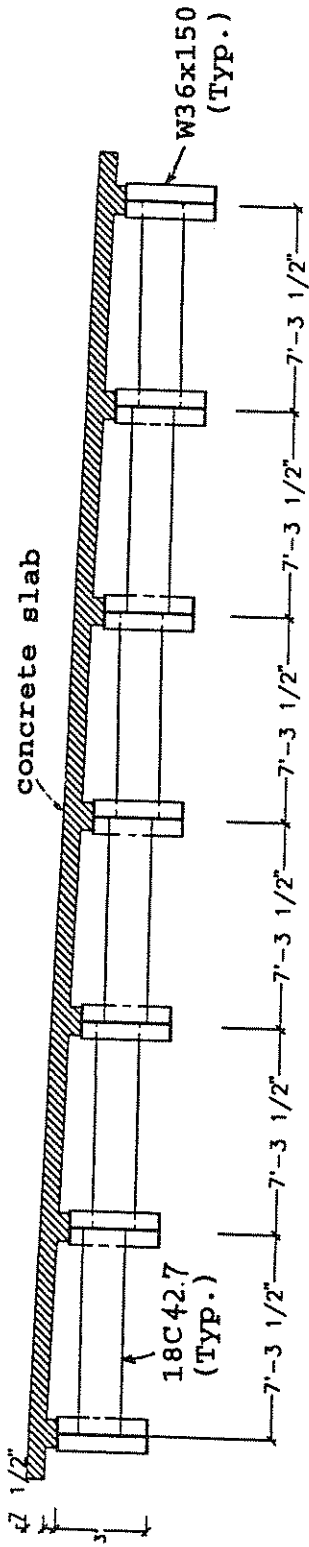


BRIDGE ELEVATION

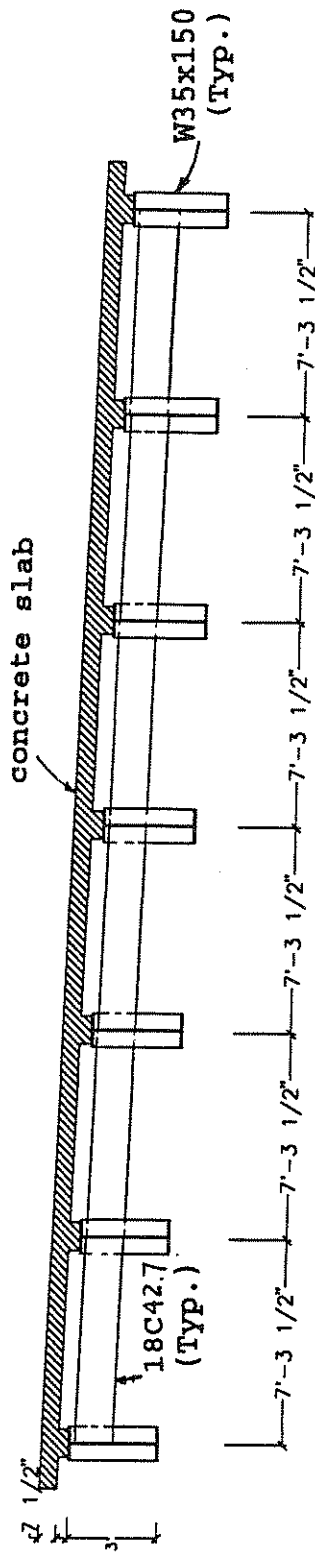


BRIDGE PLAN

Figure 2.1 South Bound Lanes of Cazenovia Creek Overpass

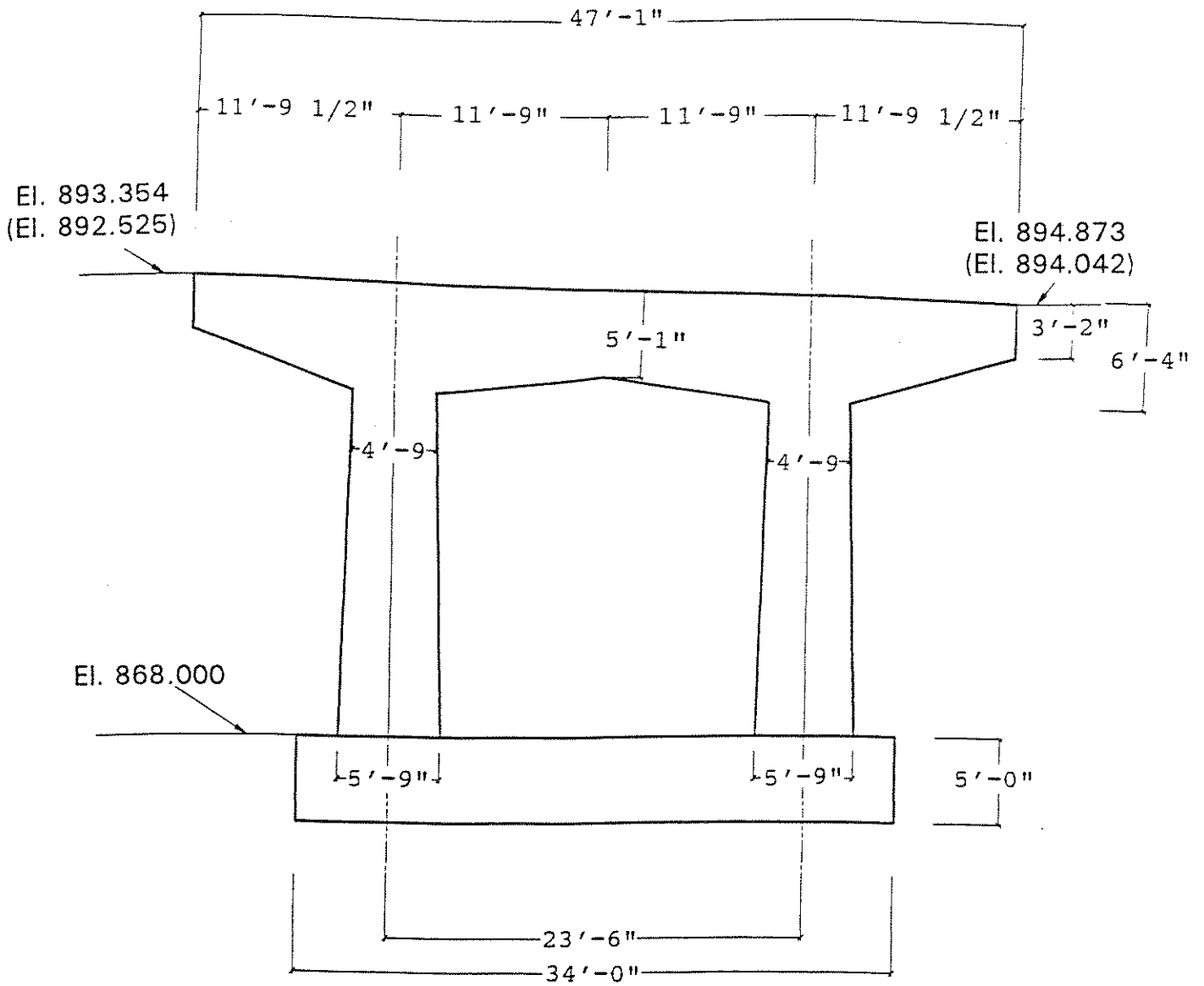


(a) Deck Section at Pier



(b) Deck Section at Abutment

Figure 2.2 Deck Section of South Bound Lane



number in () for S. pier

Figure 2.3 Pier Bent Elevation of South Bound Lane

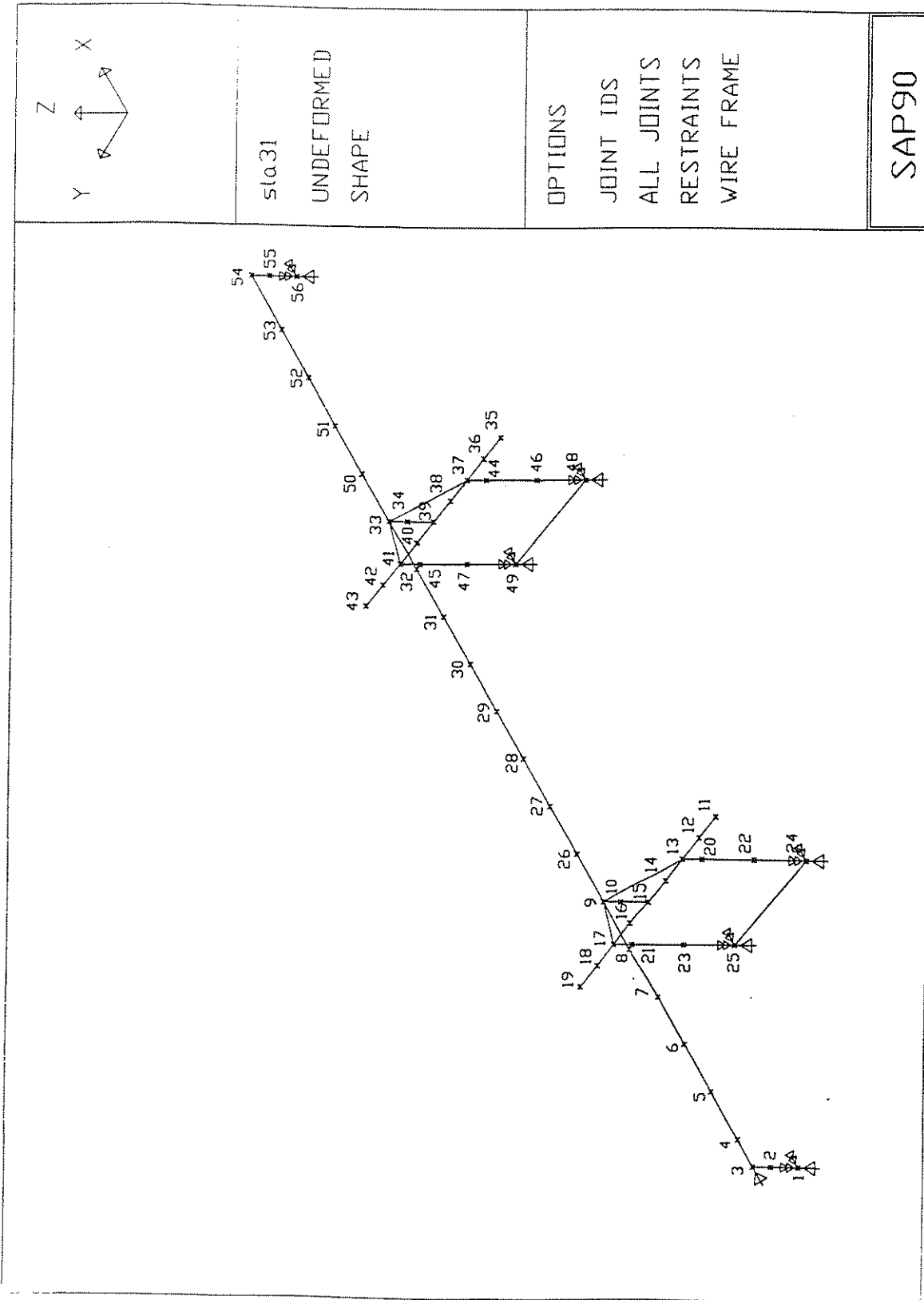


Figure 3.1 3-Dimensional Model of South Bound Lane

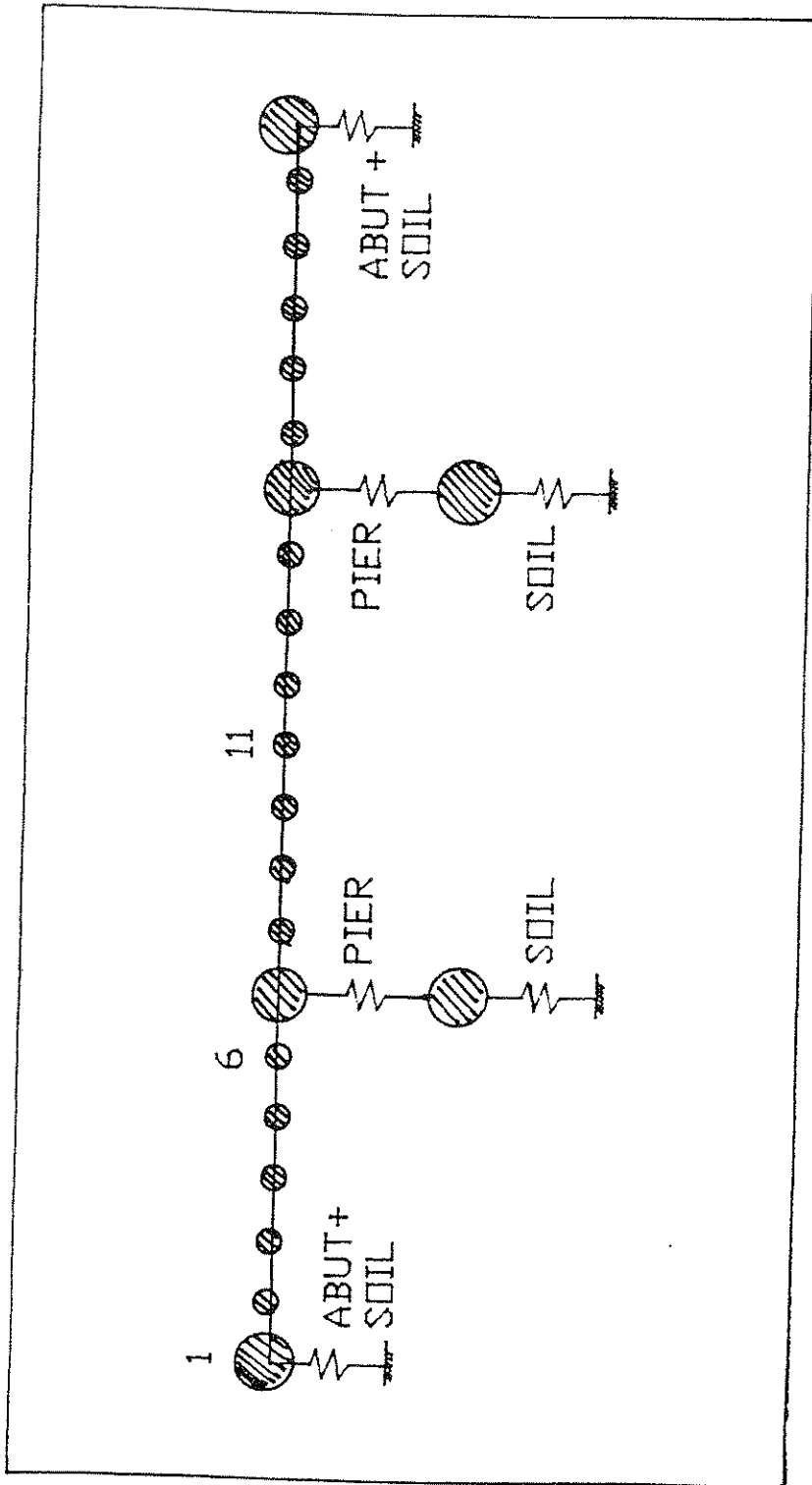


Figure 4.1 2-Dimensional Simple Model of South Bound Lane

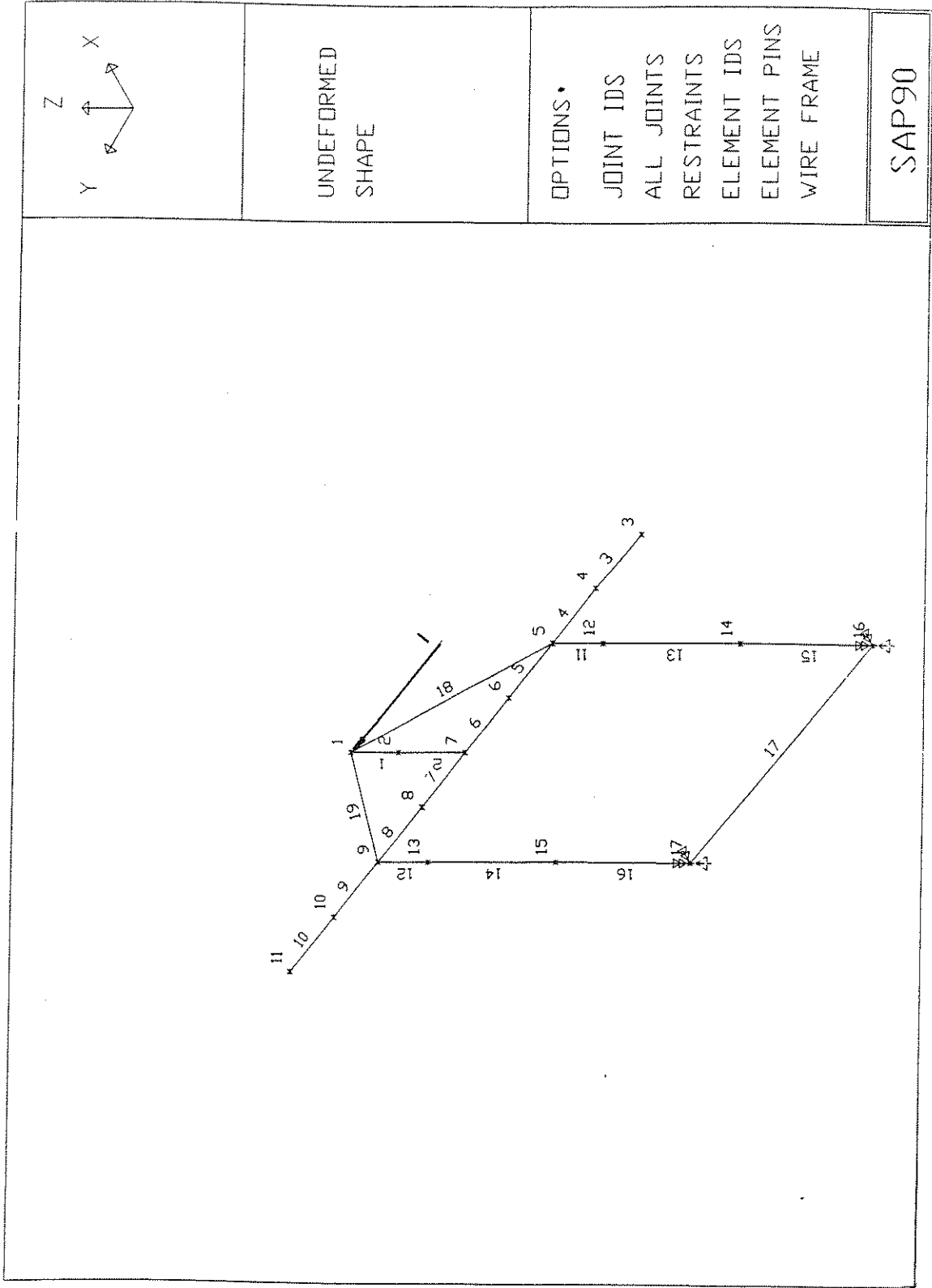


Figure 4.2 Pier Model for Equivalent Spring Stiffness

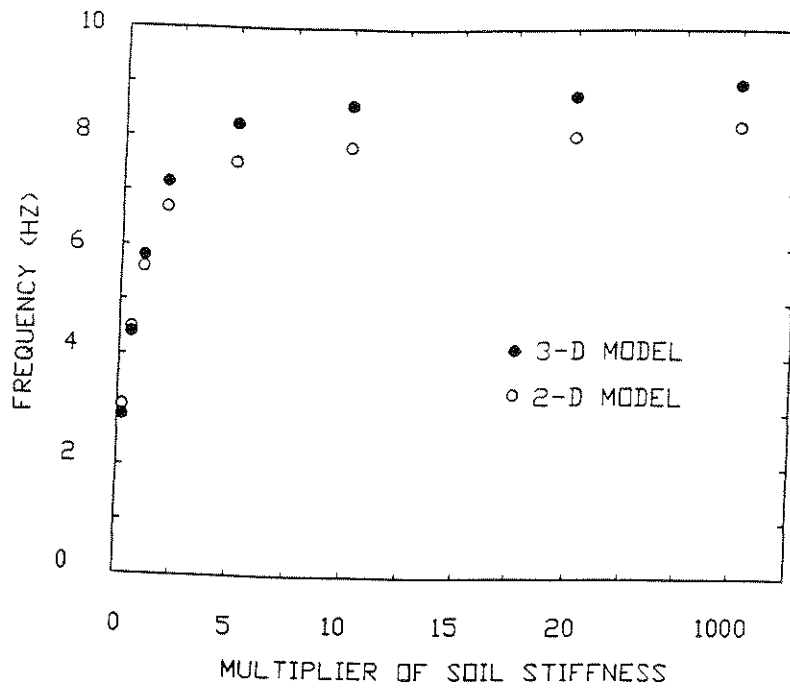


Figure 5.1 Soil Stiffness vs. Fundamental Frequencies

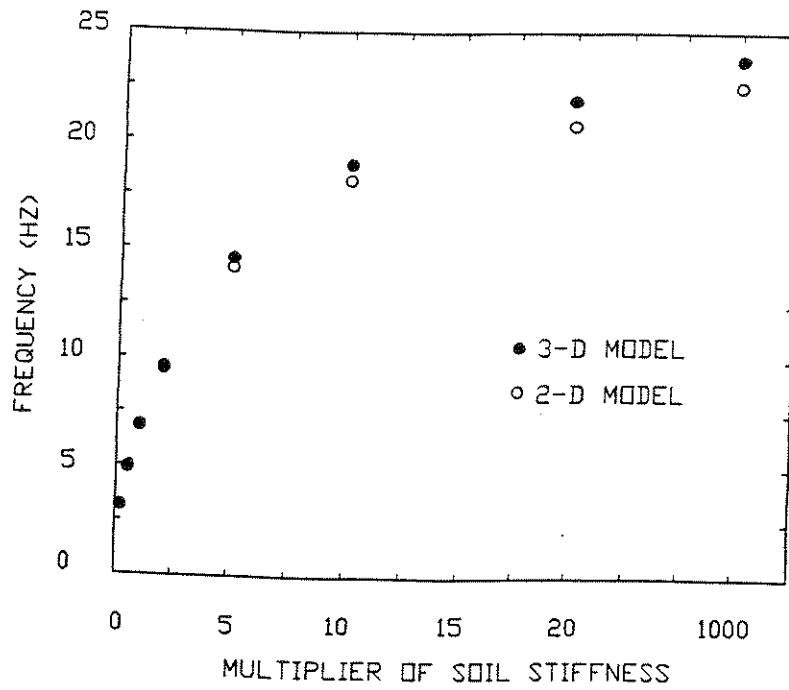


Figure 5.2 Soil Stiffness vs. Second Frequencies

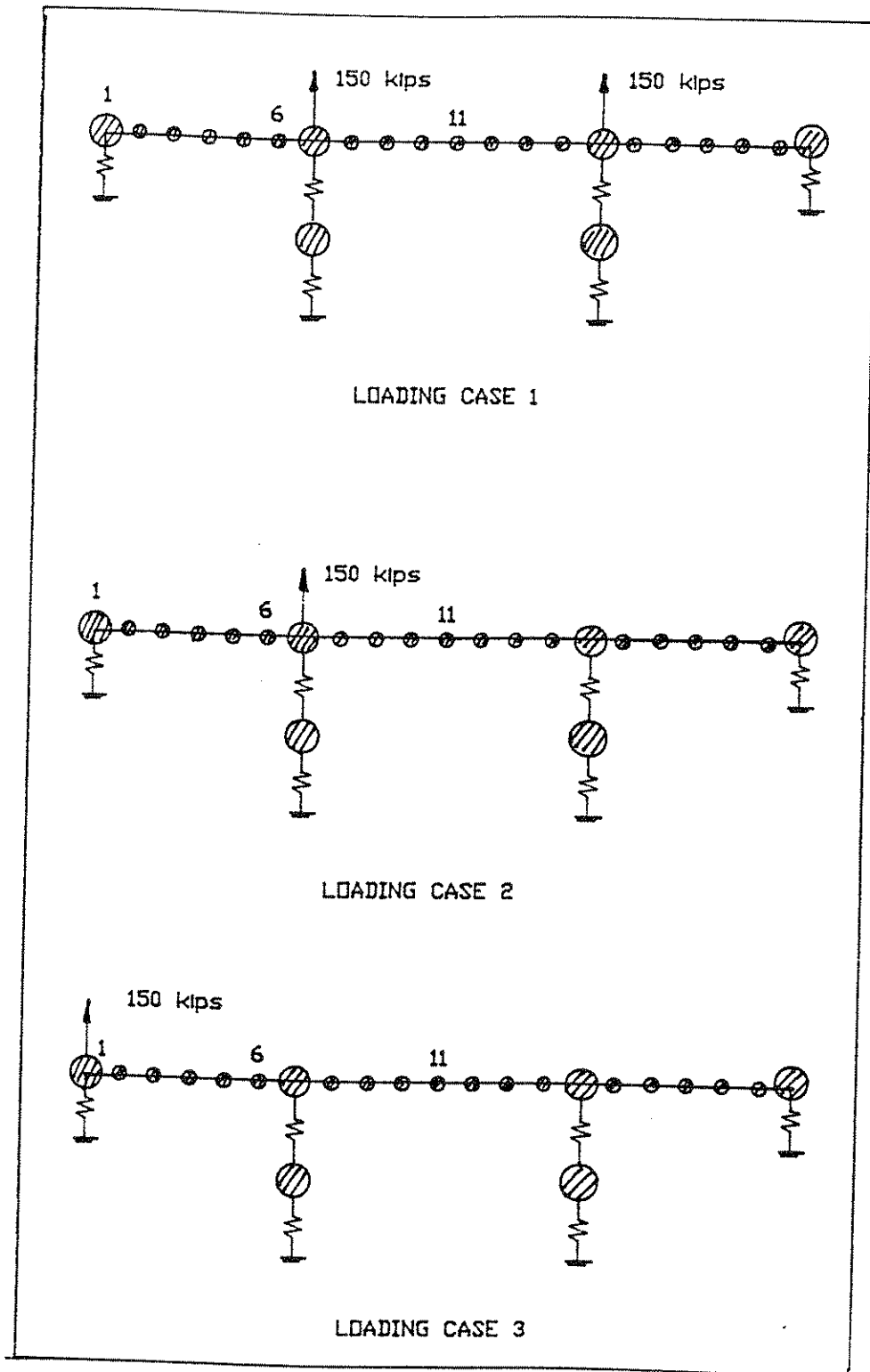


Figure 6.1 Load Cases for Pretest of Simple Model

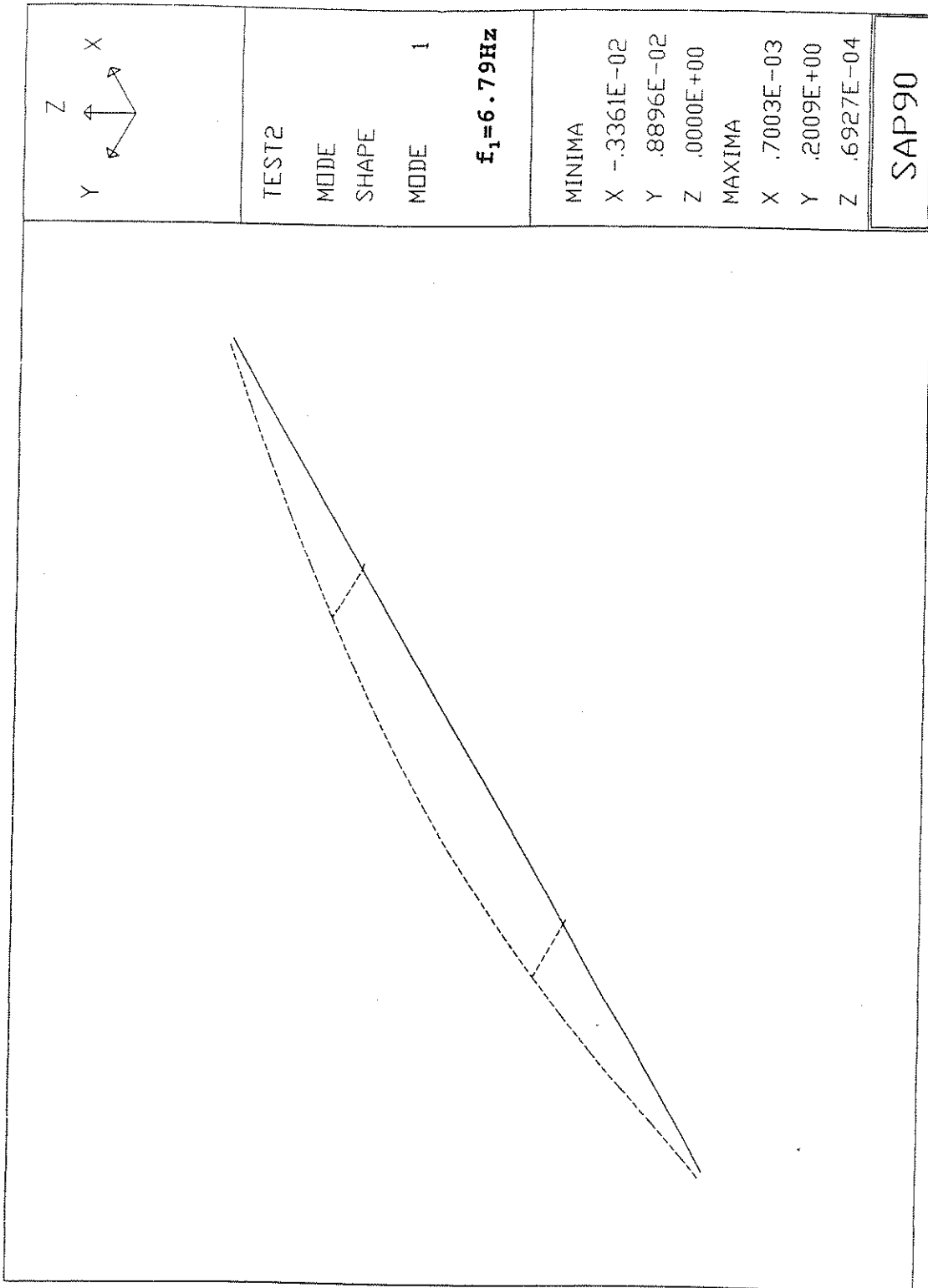


Figure 6.2 The First Transverse Mode Shape of Simple Model

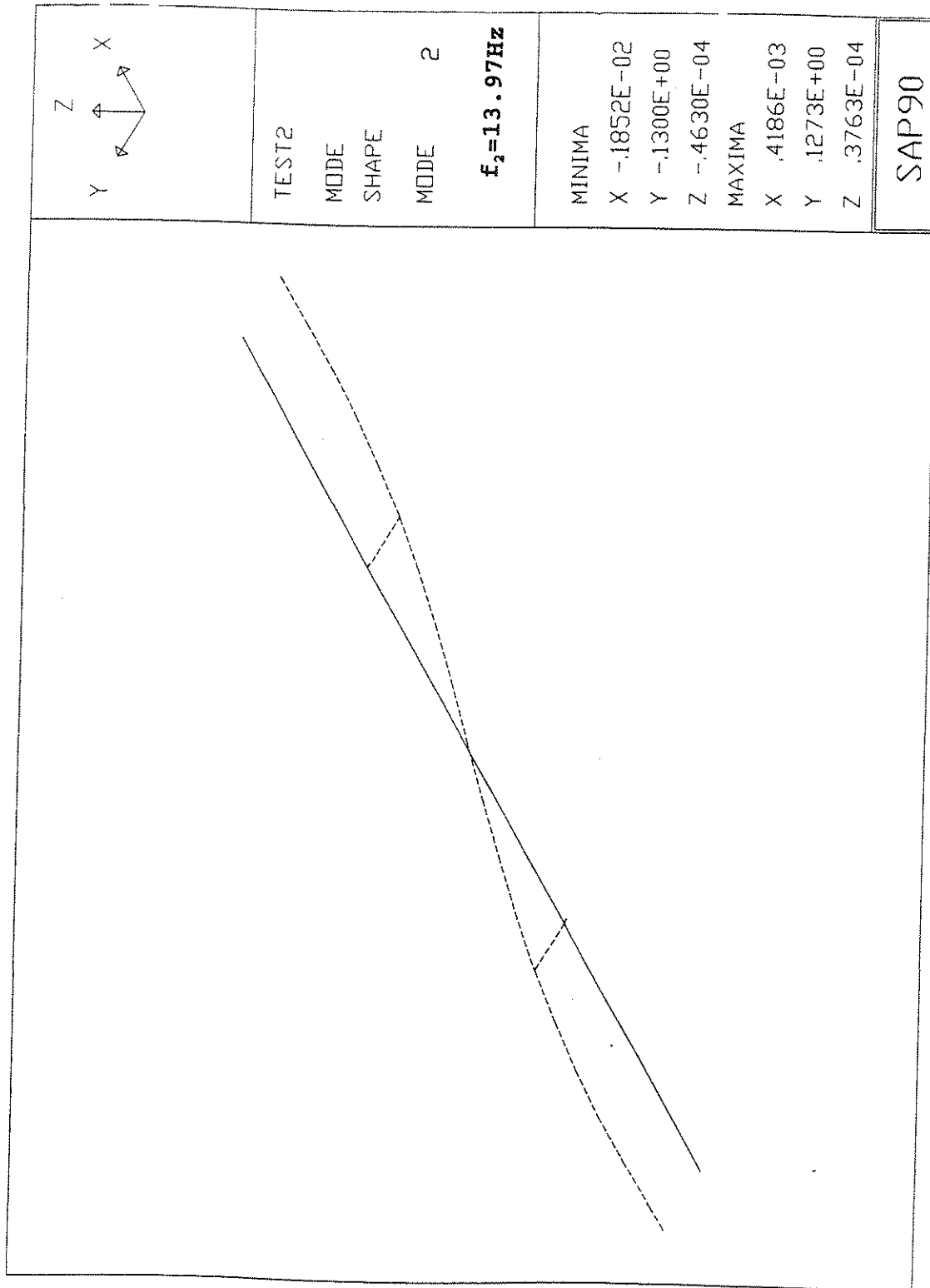


Figure 6.3 The Second Transverse Mode Shape of Simple Model

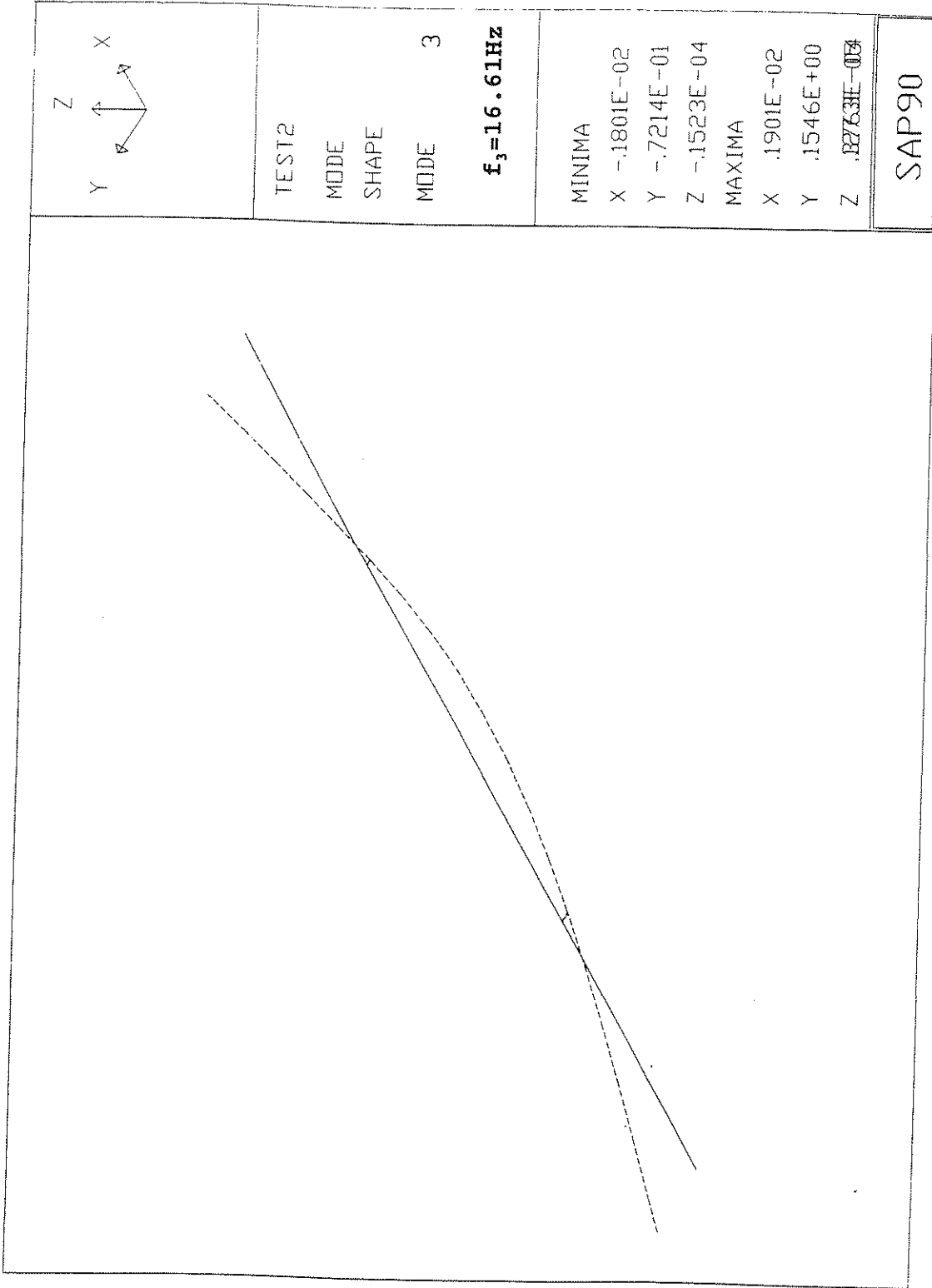


Figure 6.4 The Third Transverse Mode Shape of Simple Model

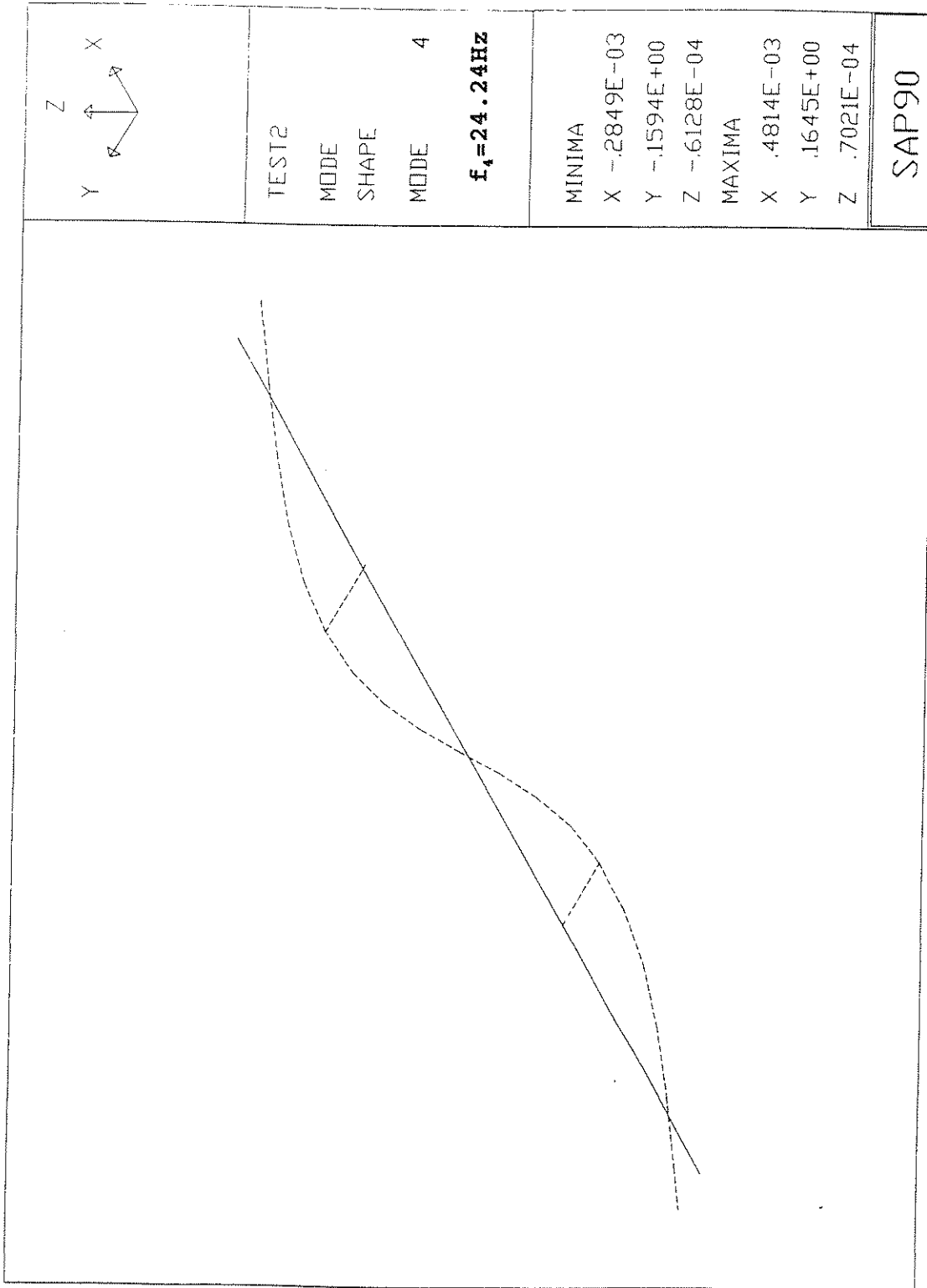


Figure 6.5 The Fourth Transverse Mode Shape of Simple Model

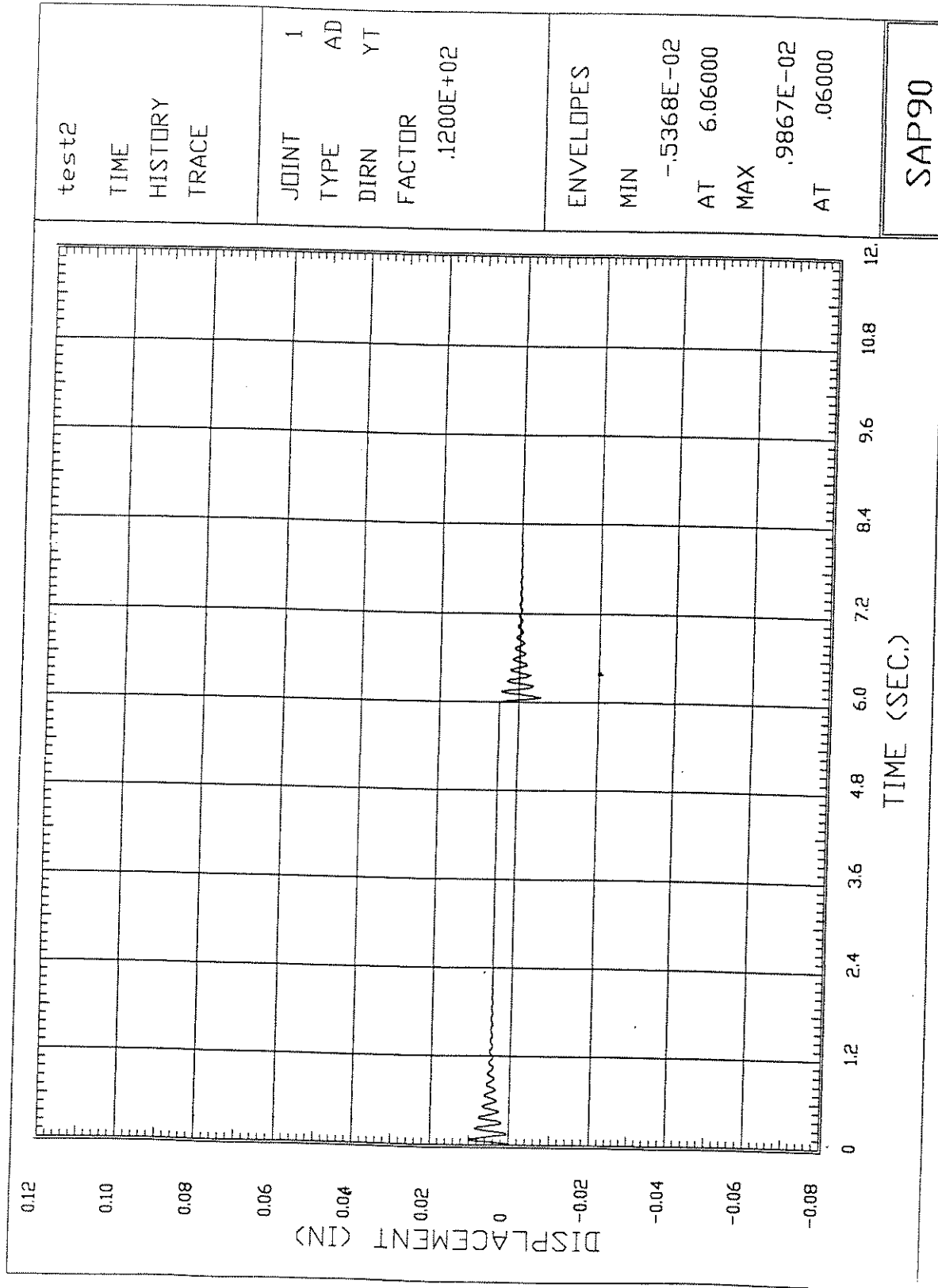


Figure 6.6 Displacement at Joint 1 in Load Case 1

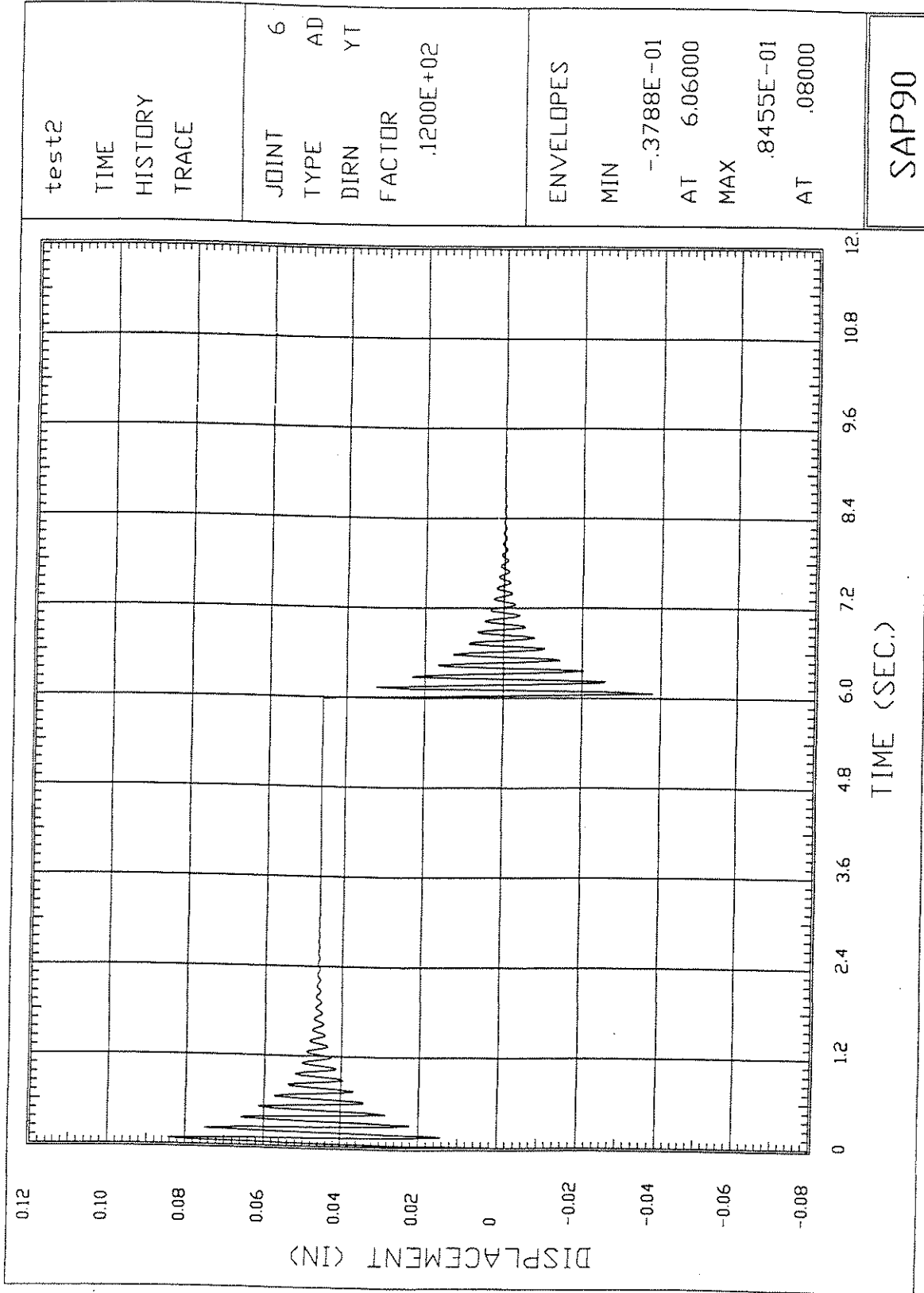


Figure 6.7 Displacement at Joint 6 in Load Case 1

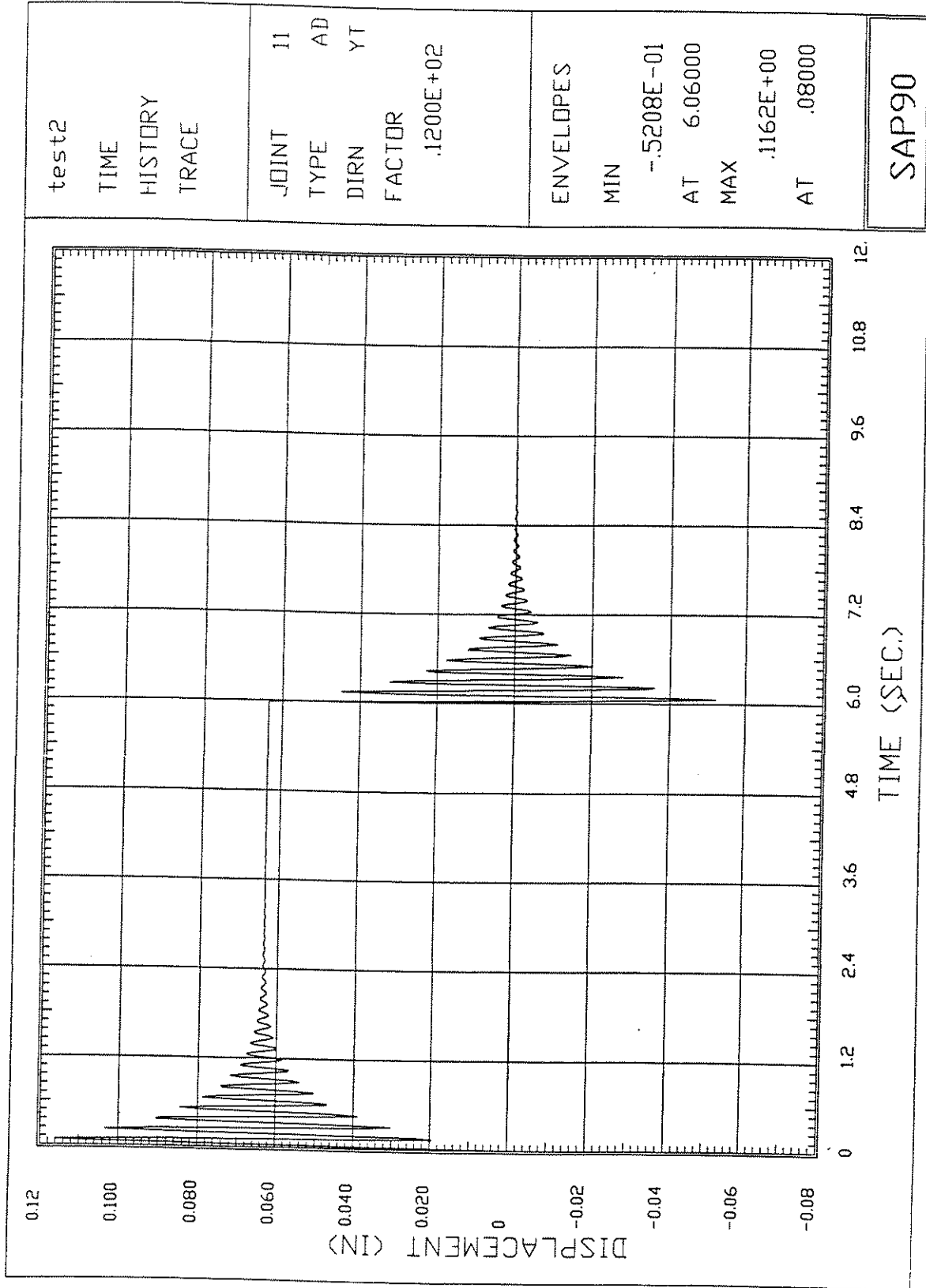


Figure 6.8 Displacement at Joint 11 in Load Case 1

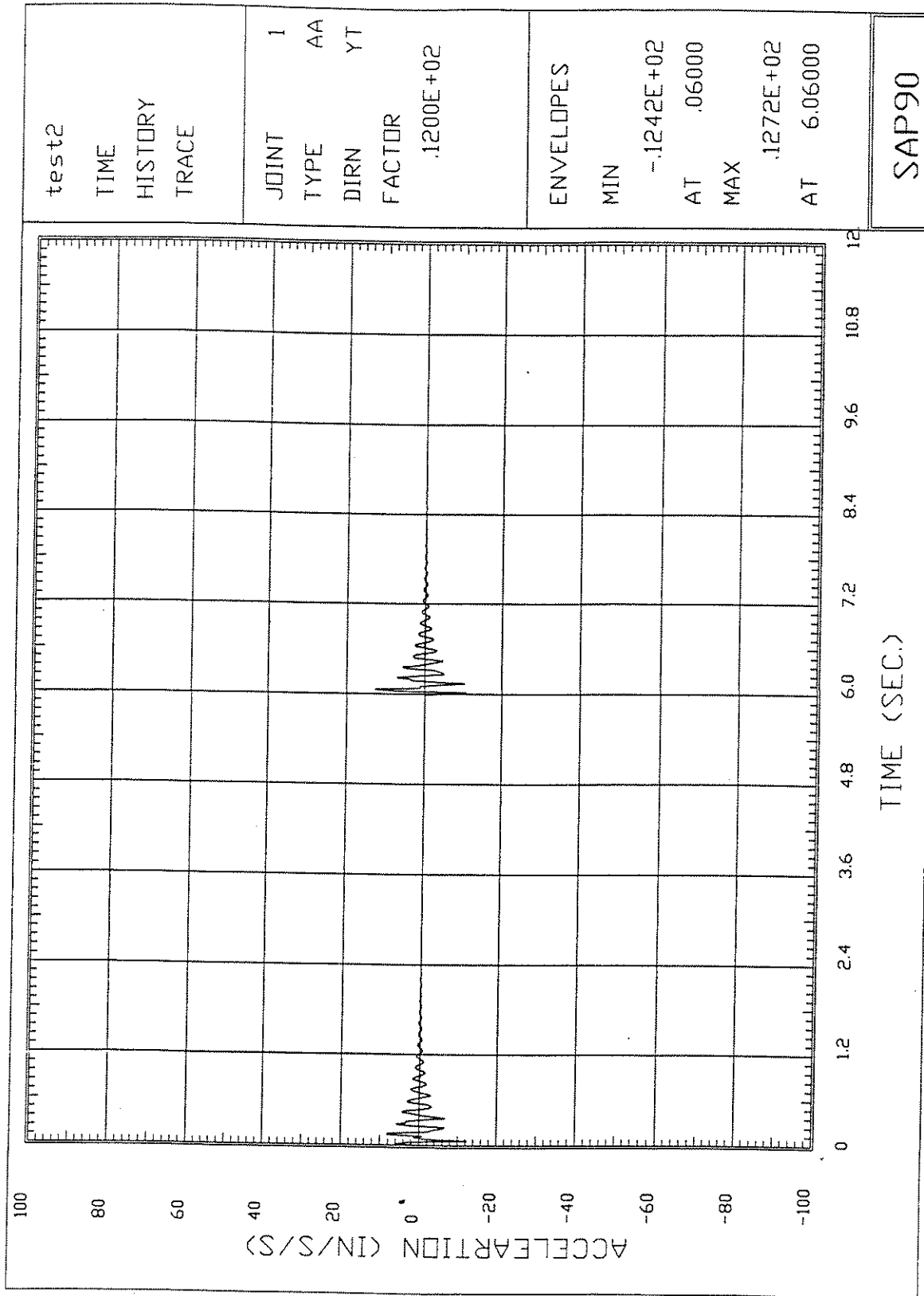


Figure 6.9 Acceleration at Joint 1 in Load Case 1

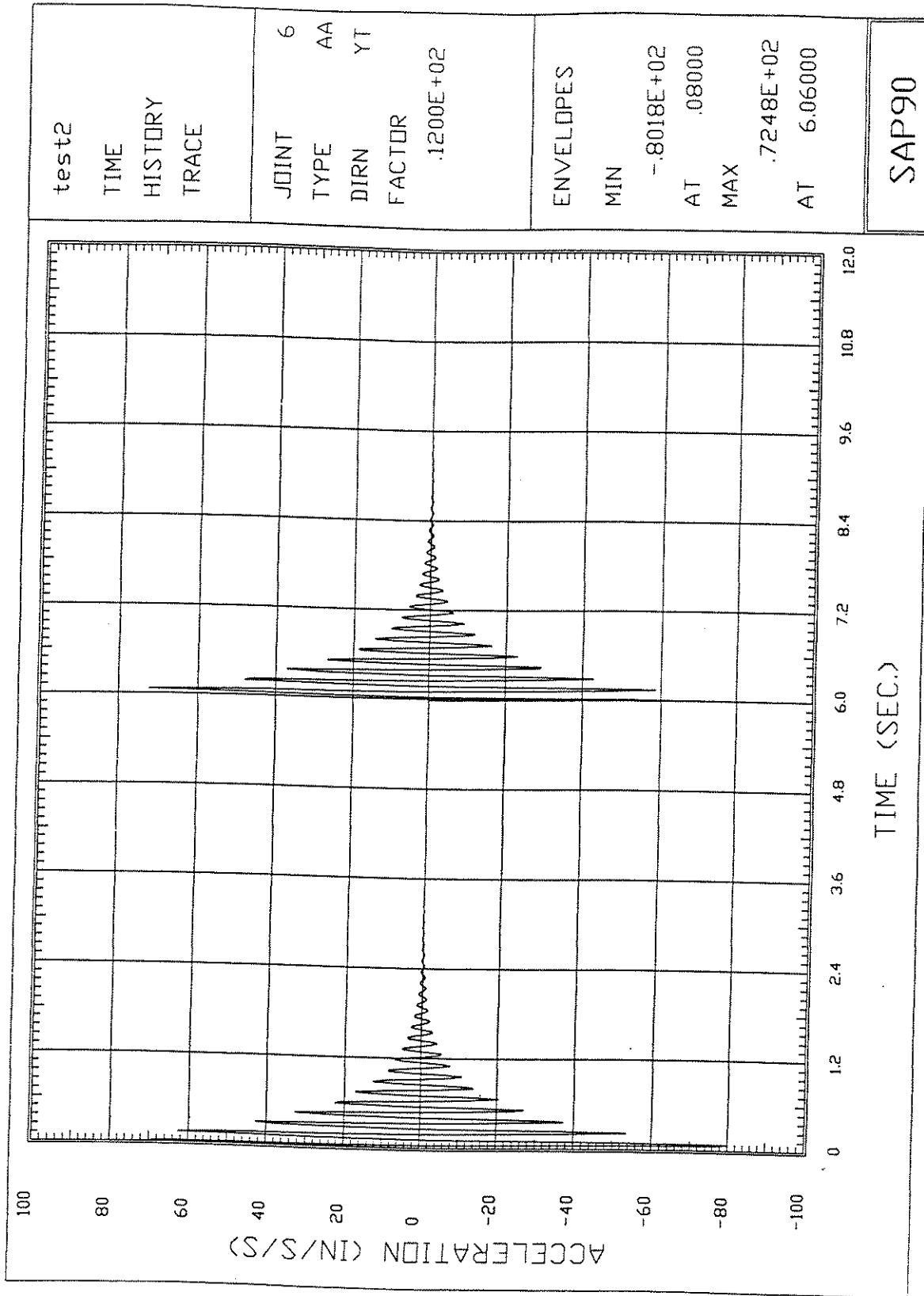


Figure 6.10 Acceleration at Joint 6 in Load Case 1

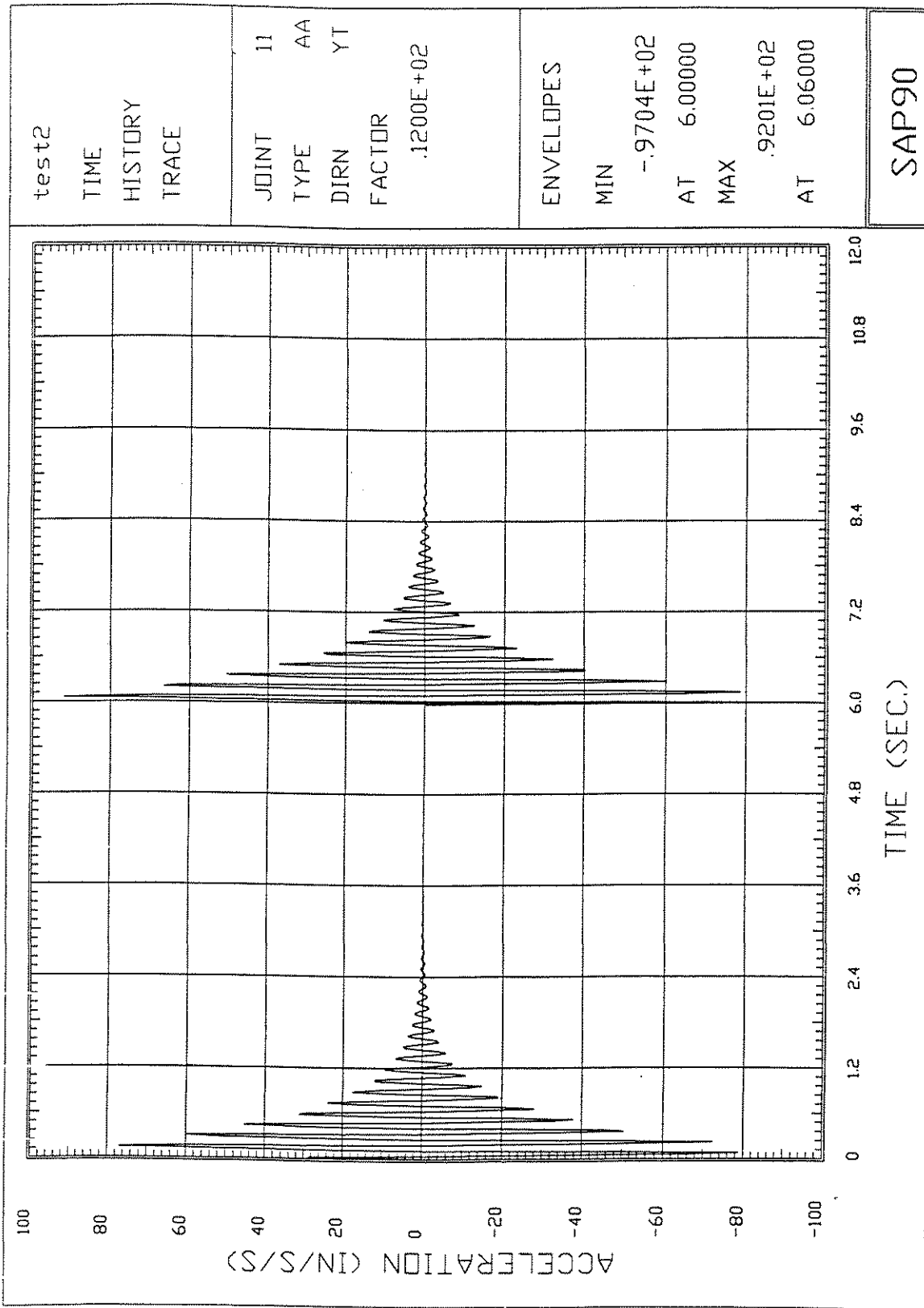


Figure 6.11 Acceleration at Joint 11 in Load Case 1

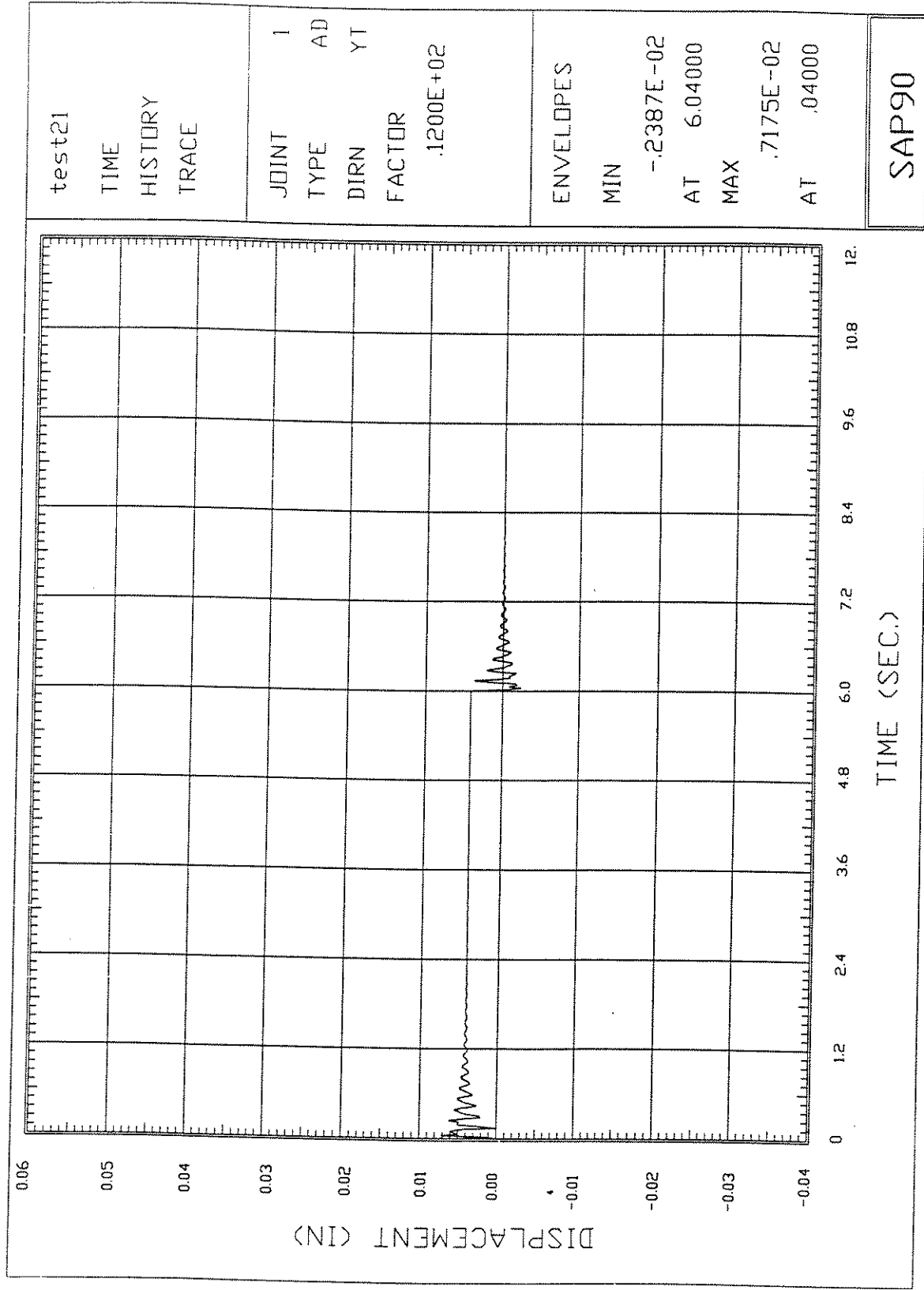


Figure 6.12 Displacement at Joint 1 in Load Case 2

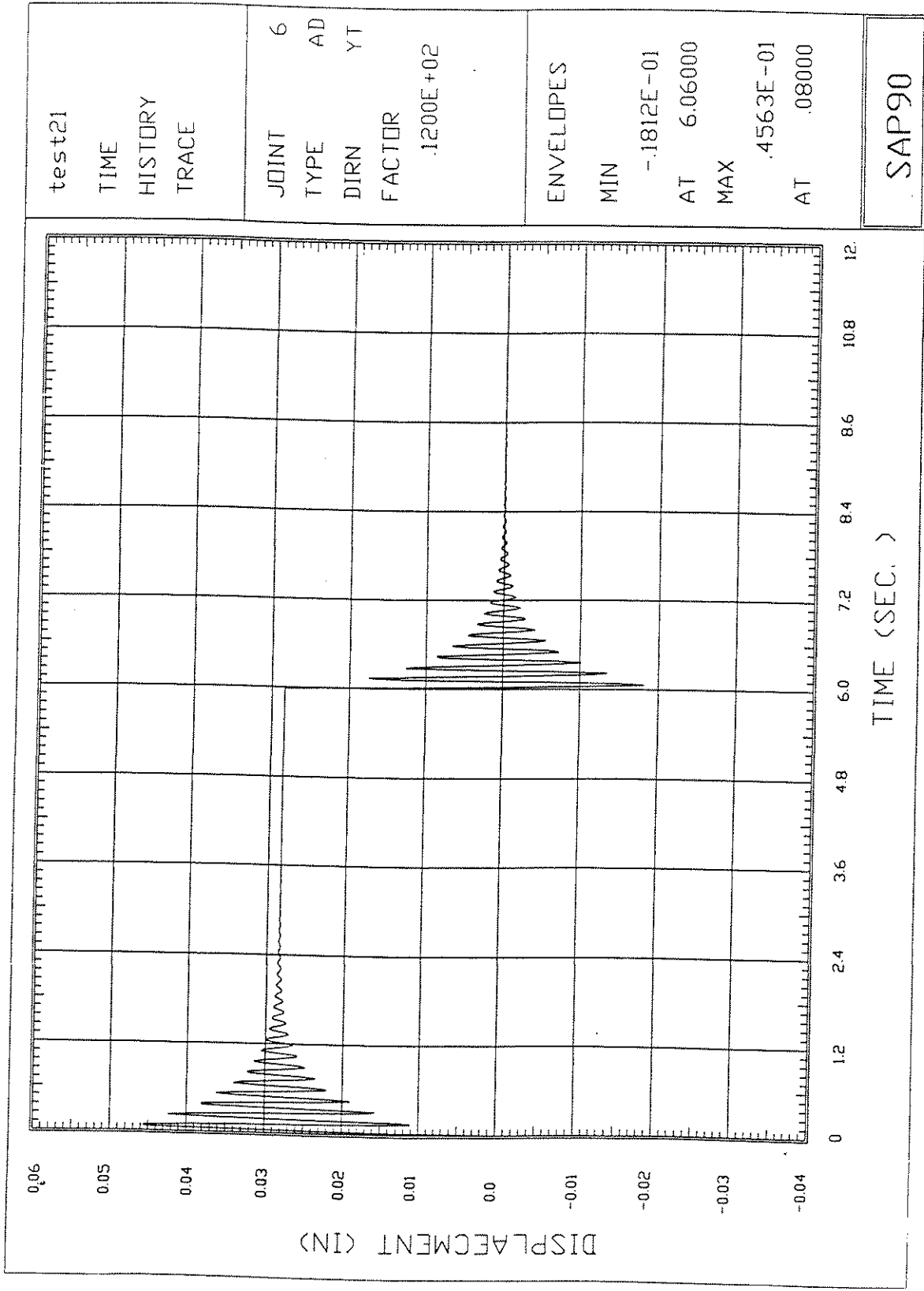


Figure 6.13 Displacement at Joint 6 in Load Case 2

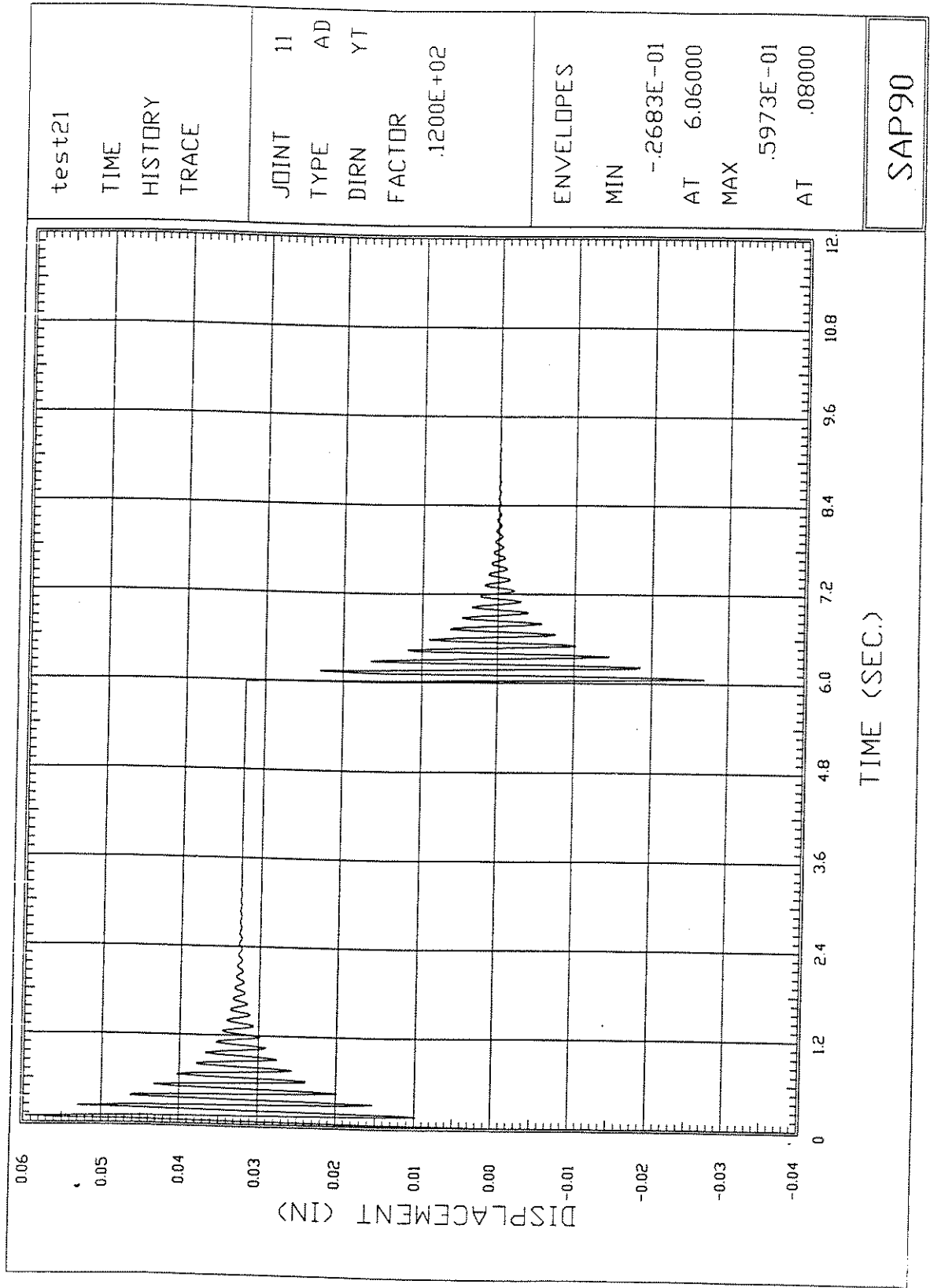


Figure 6.14 Displacement at Joint 11 in Load Case 2

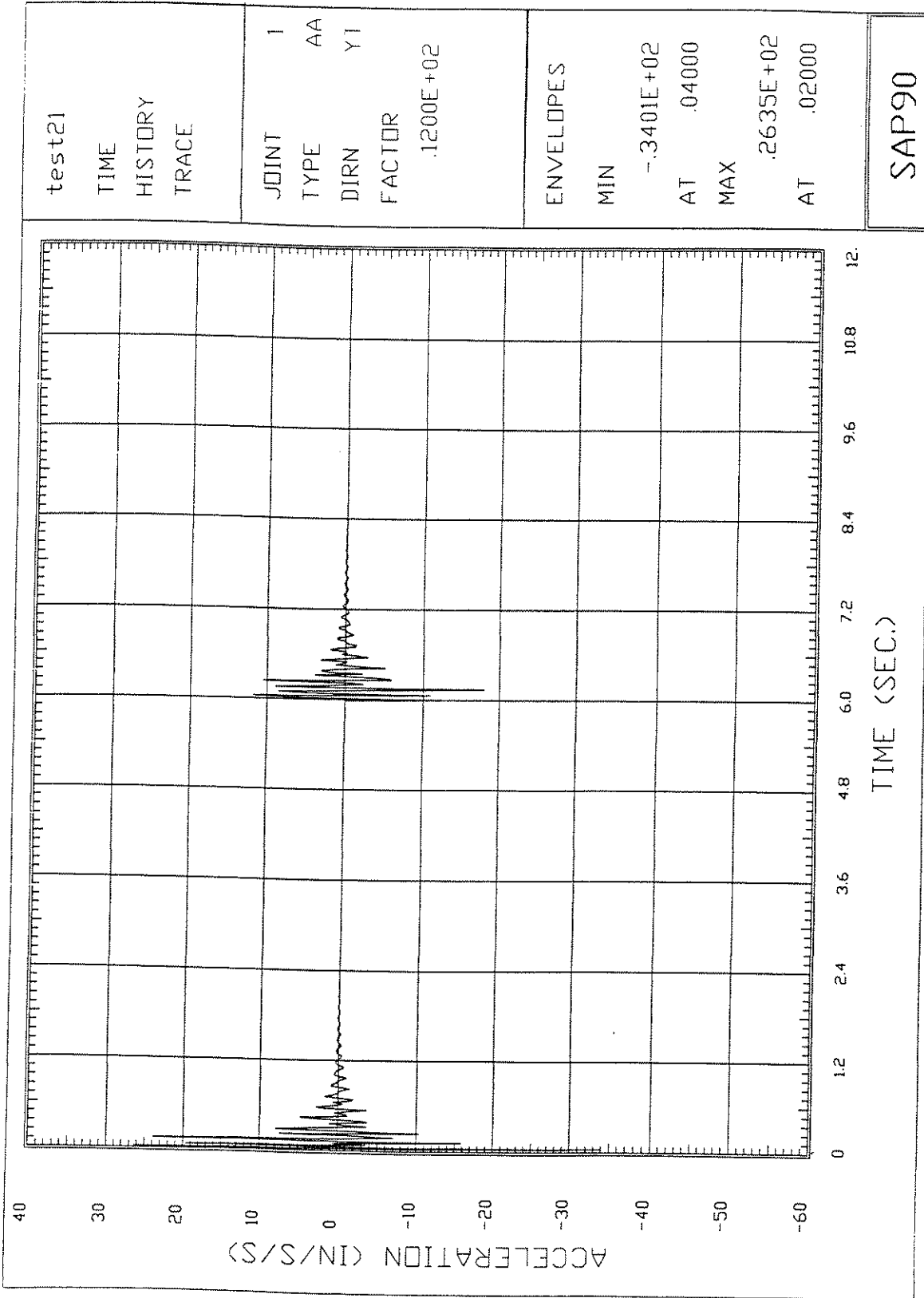


Figure 6.15 Acceleration at Joint 1 in Load Case 2

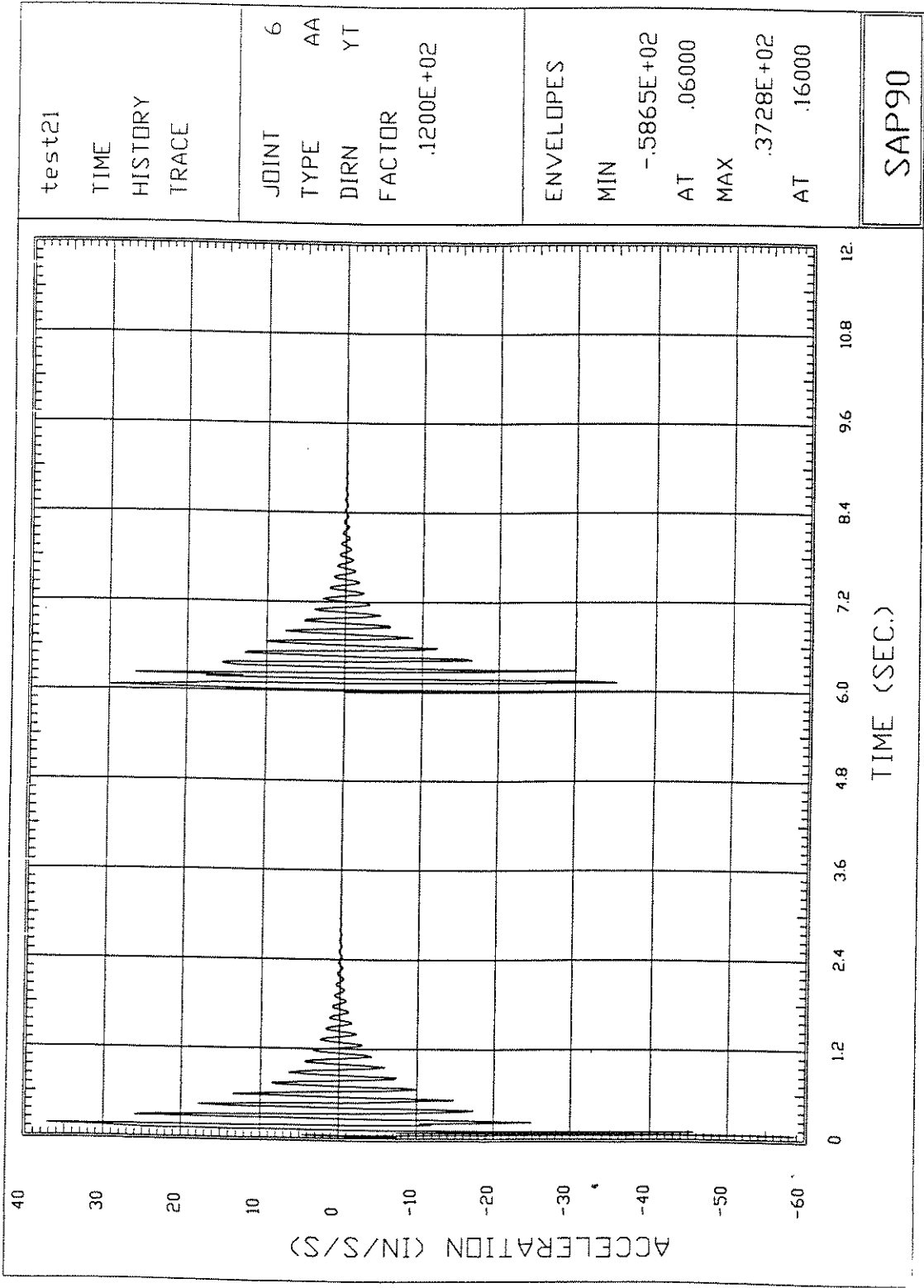


Figure 6.16 Acceleration at Joint 6 in Load Case 2

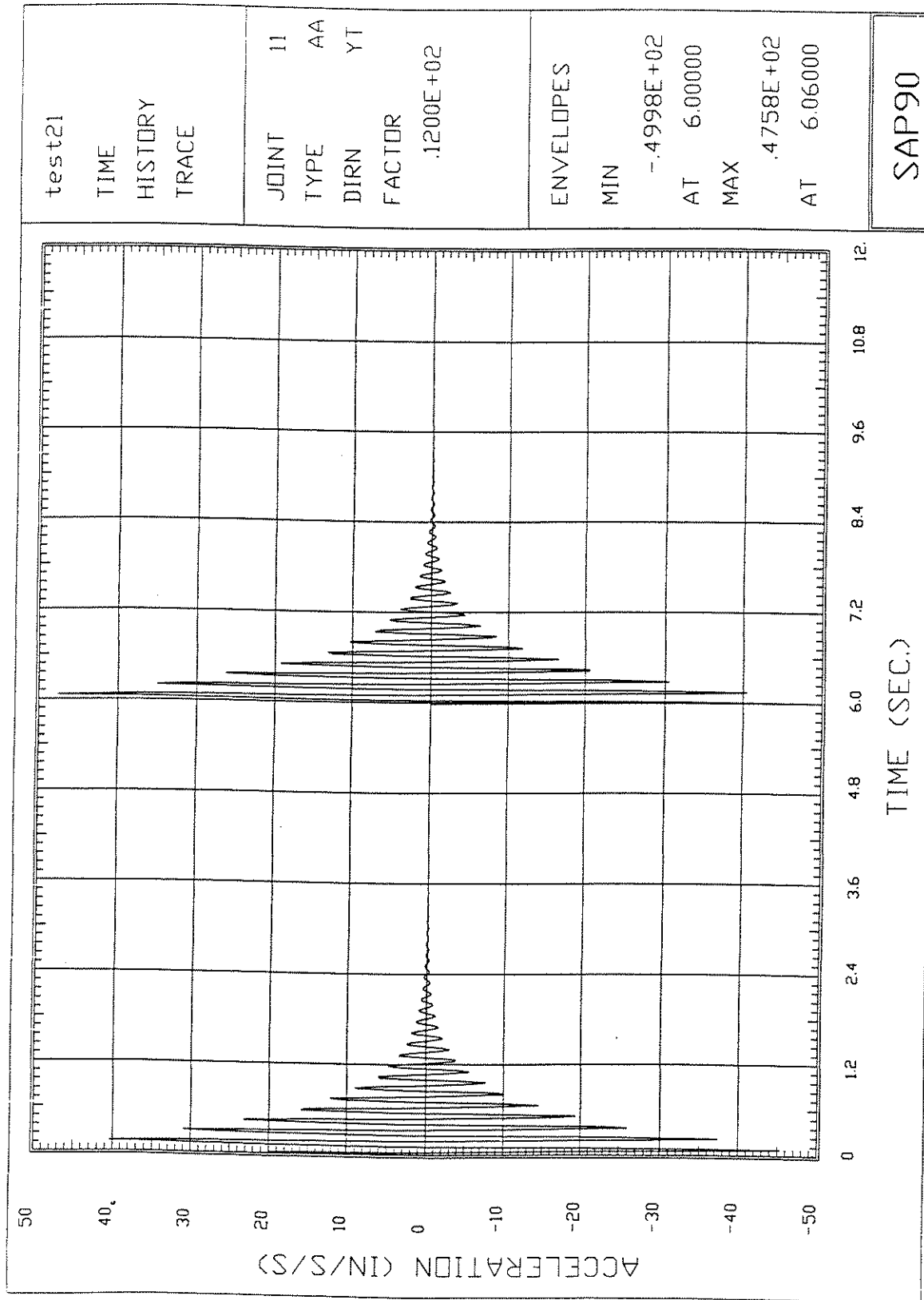


Figure 6.17 Acceleration at Joint 11 in Load Case 2

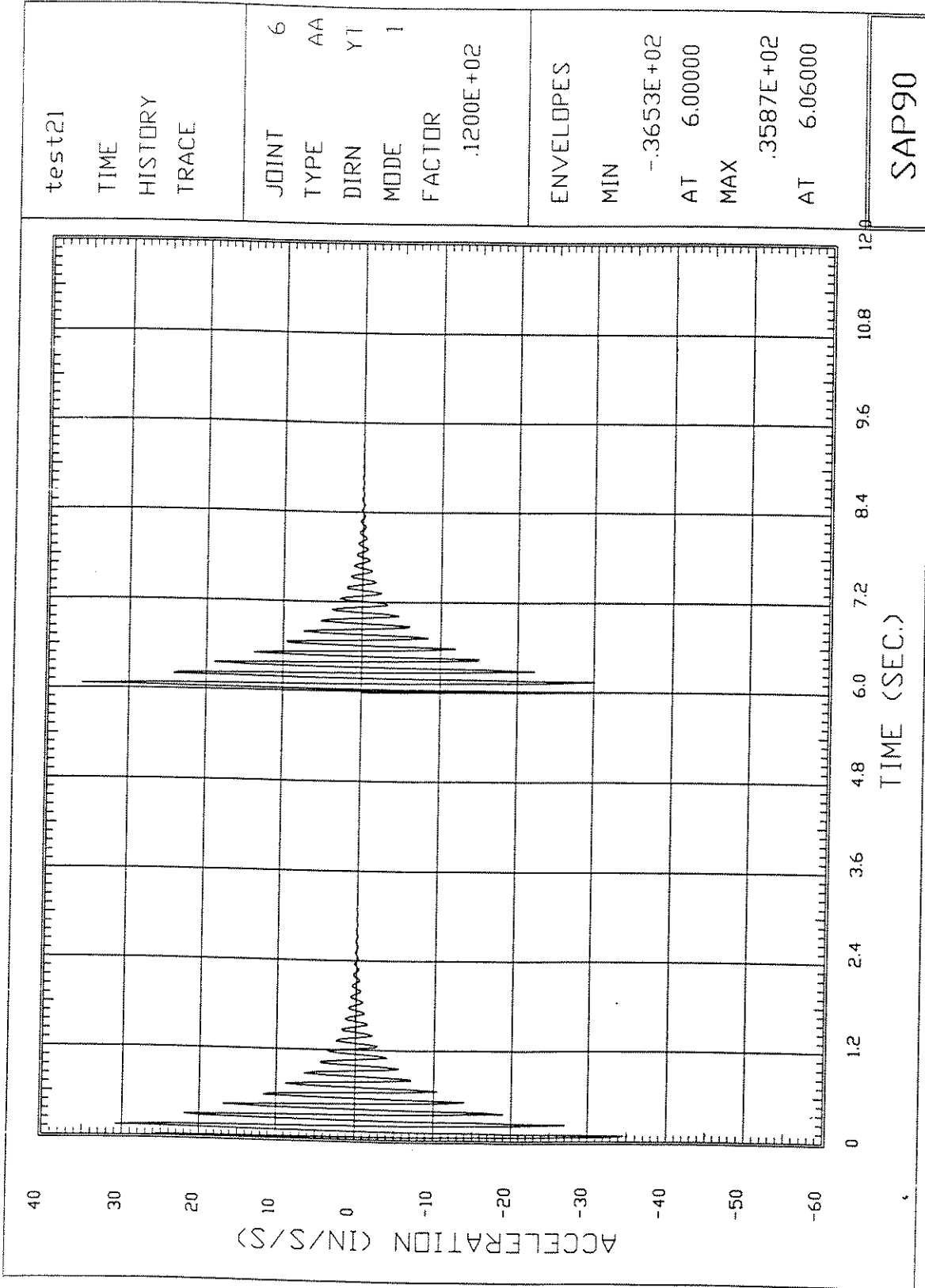


Figure 6.18 Acceleration at Joint 6 (Mode 1) in Load Case 2

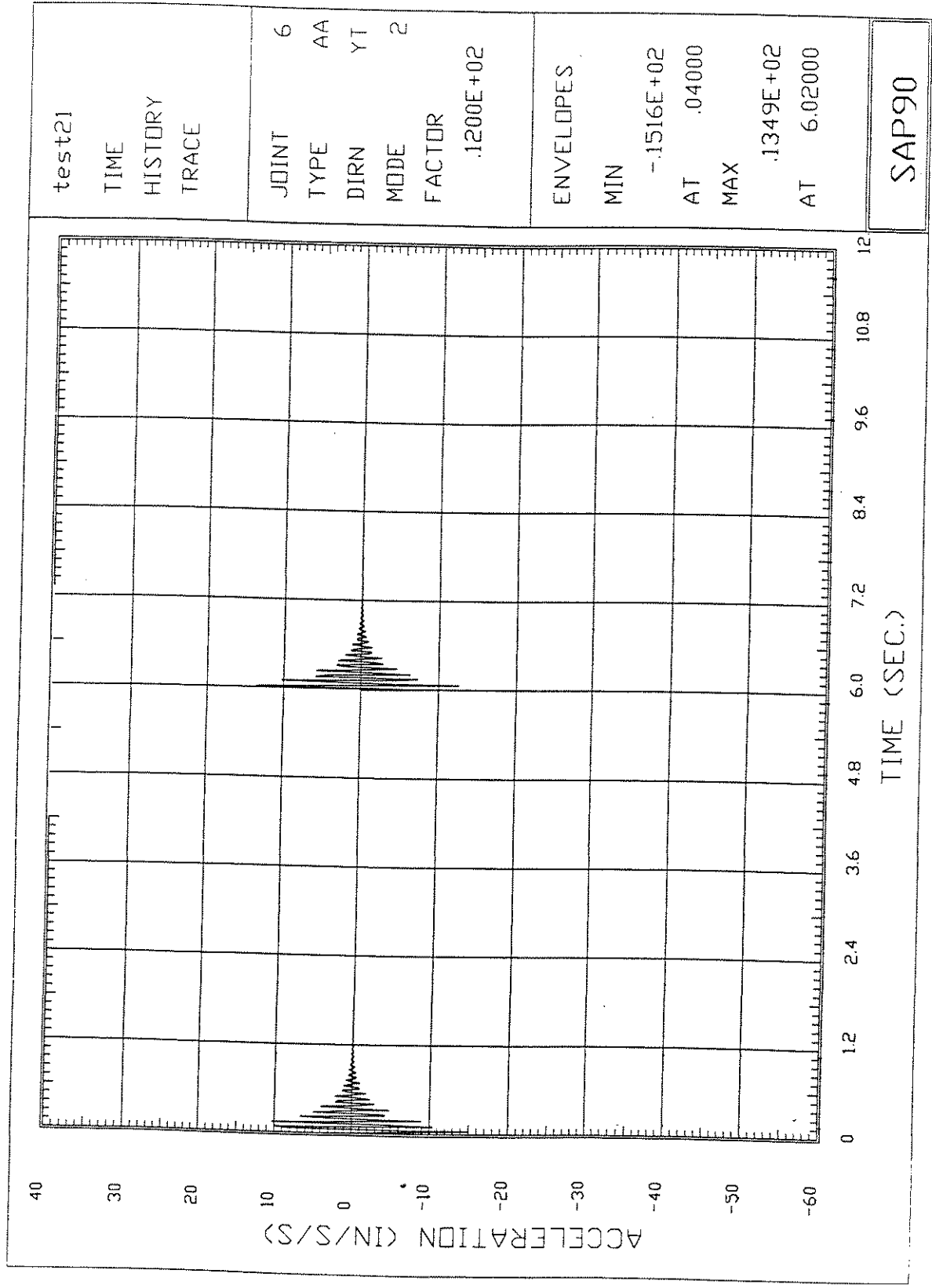


Figure 6.19 Acceleration at Joint 6 (Mode 2) in Load Case 2

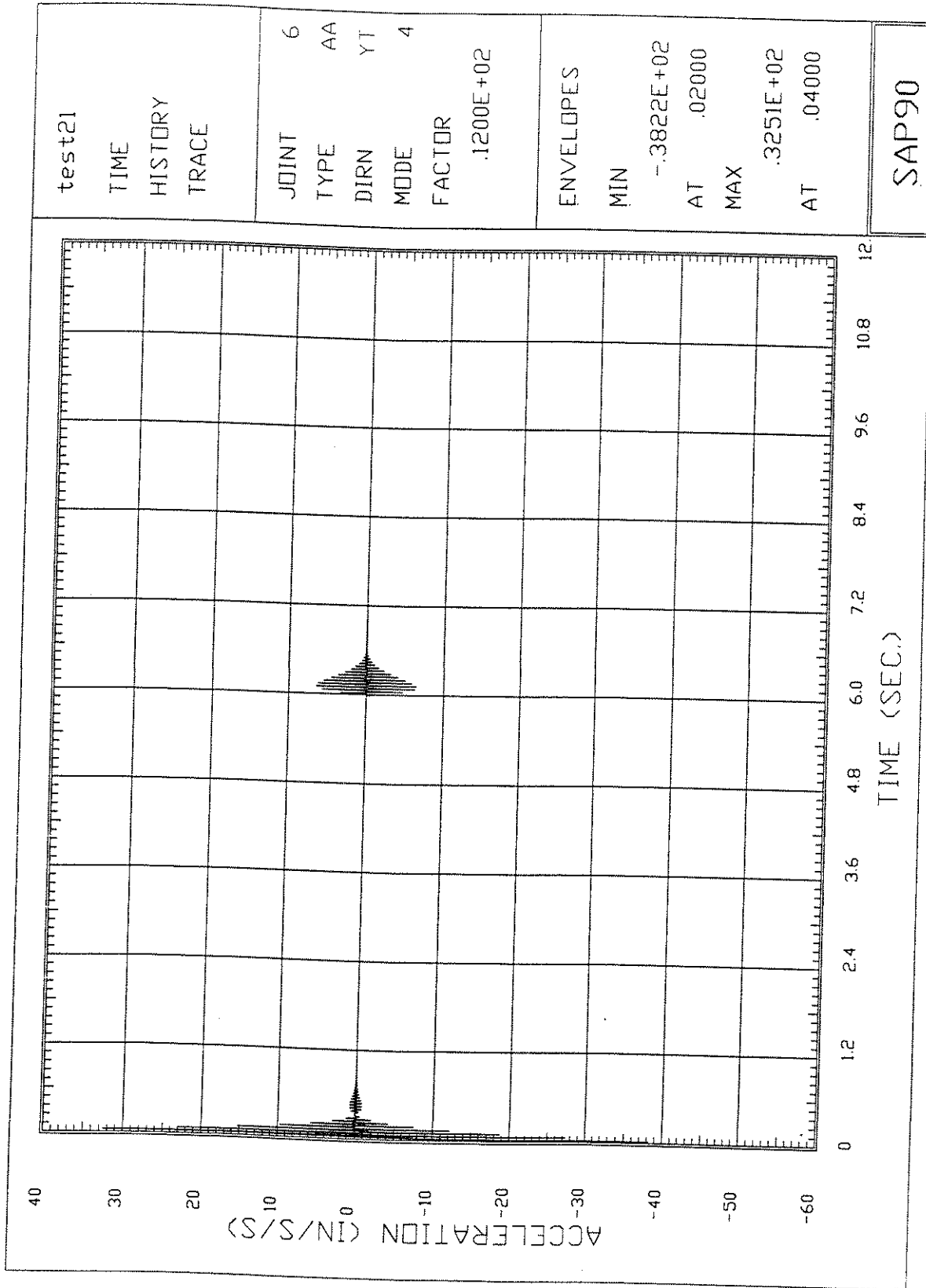
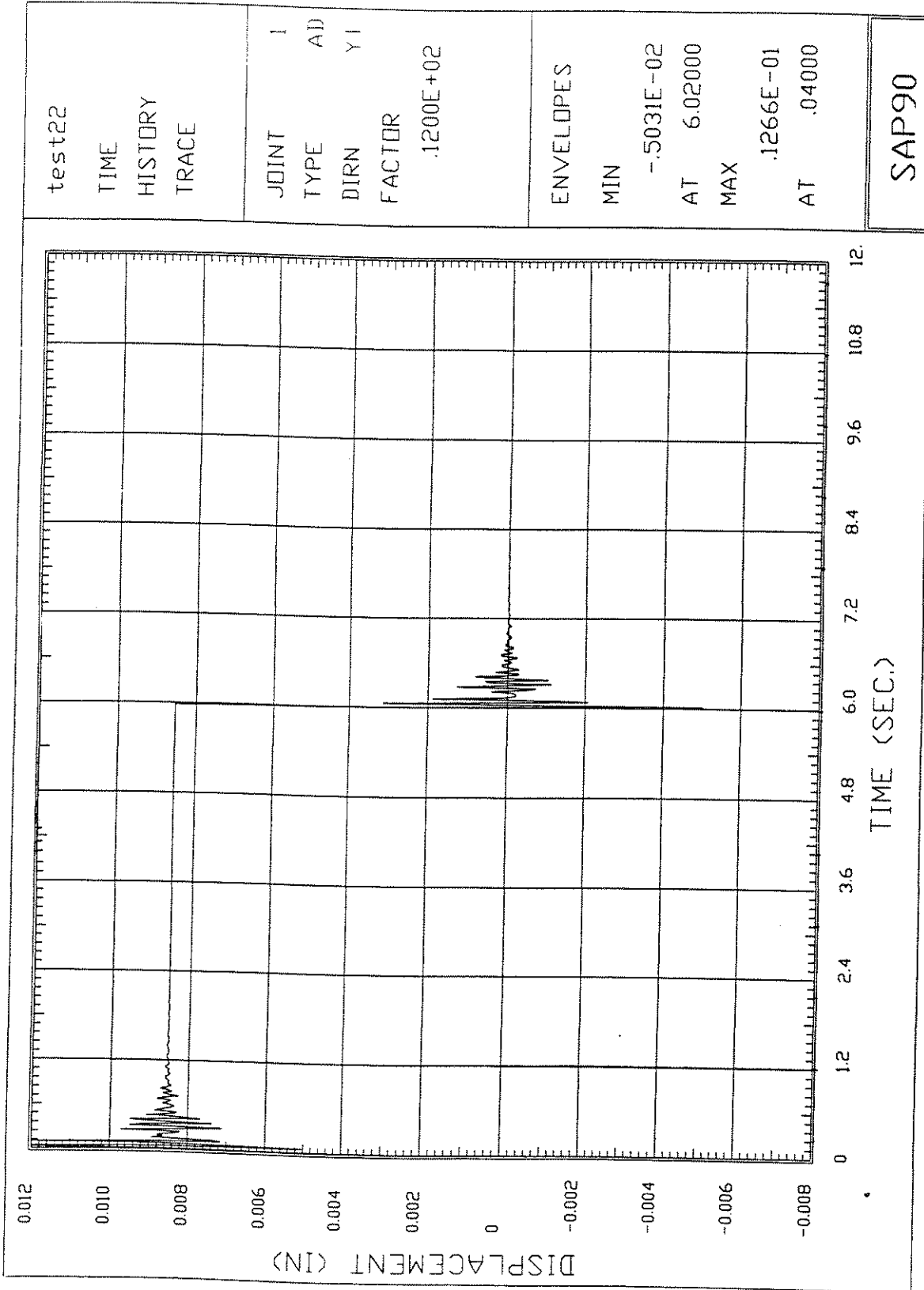


Figure 6.20 Acceleration at Joint 6 (Mode 4) in Load Case 2



test22
 TIME
 HISTORY
 TRACE

JOINT 1
 TYPE AD
 DIRN YI
 FACTOR
 .1200E+02

ENVELOPES
 MIN -.5031E-02
 AT 6.02000
 MAX .1266E-01
 AT .04000

SAP90

Figure 6.21 Displacement at Joint 1 in Load Case 3

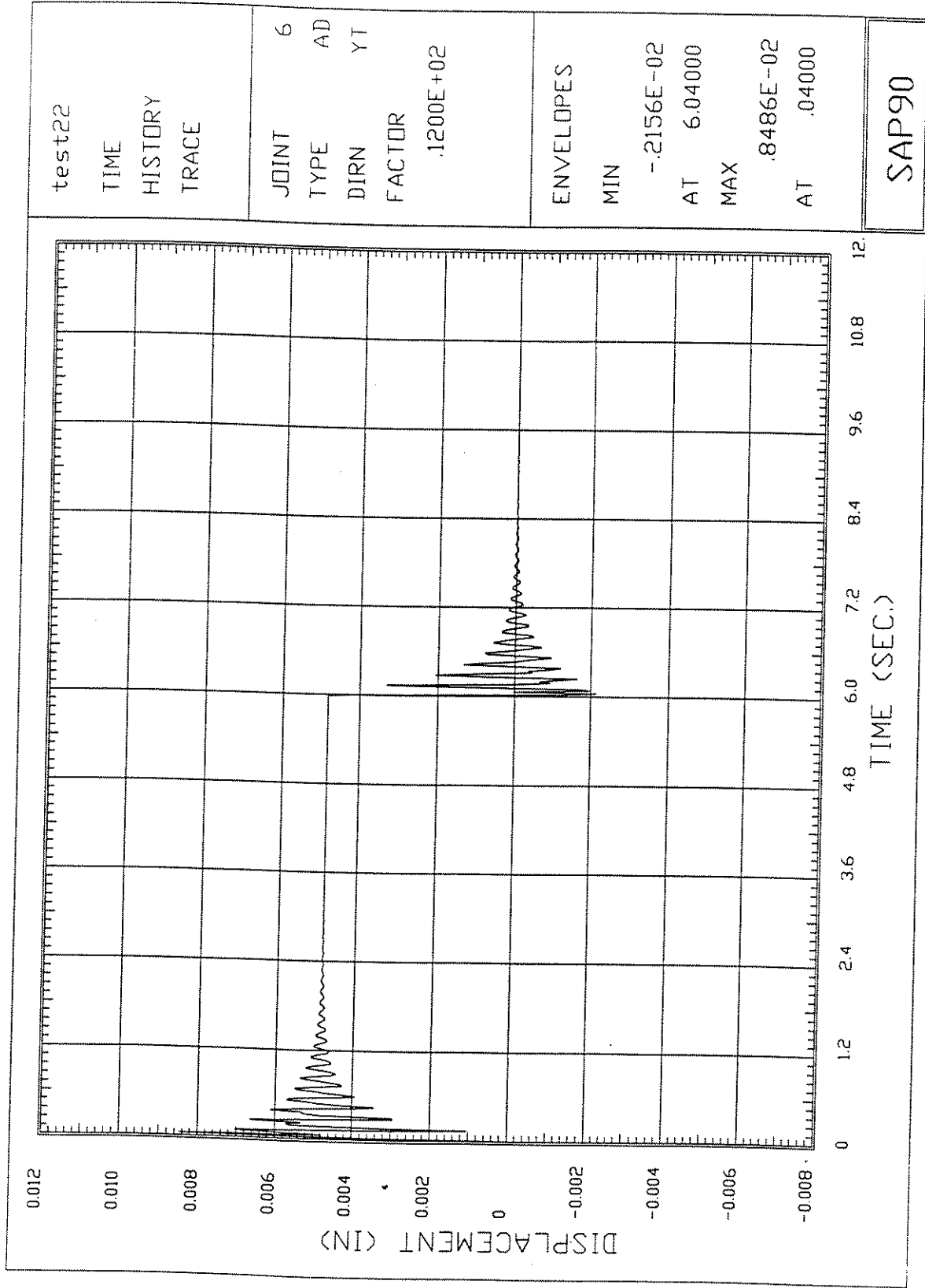


Figure 6.22 Displacement at Joint 6 in Load Case 3

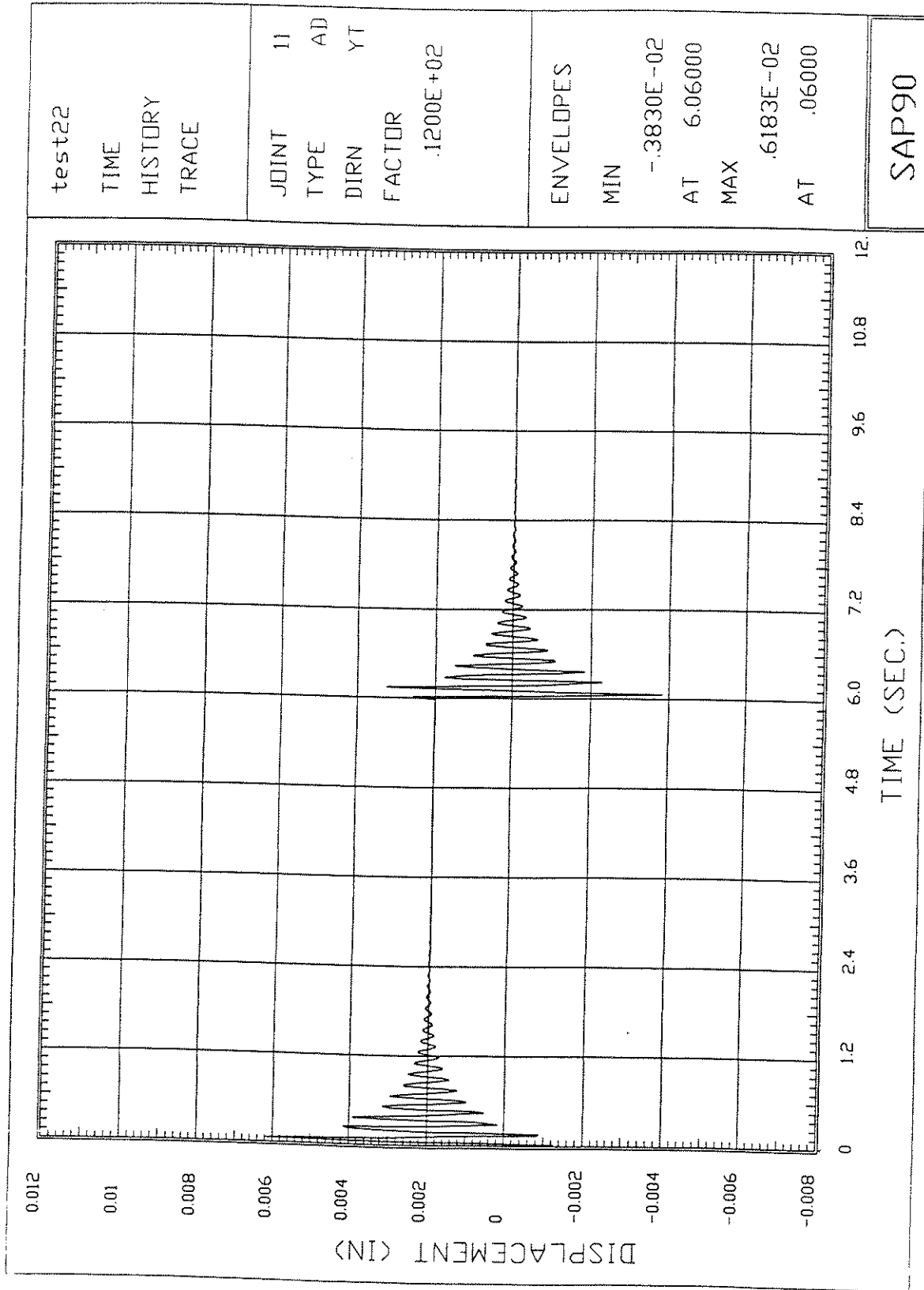


Figure 6.23 Displacement at Joint 11 in Load Case 3

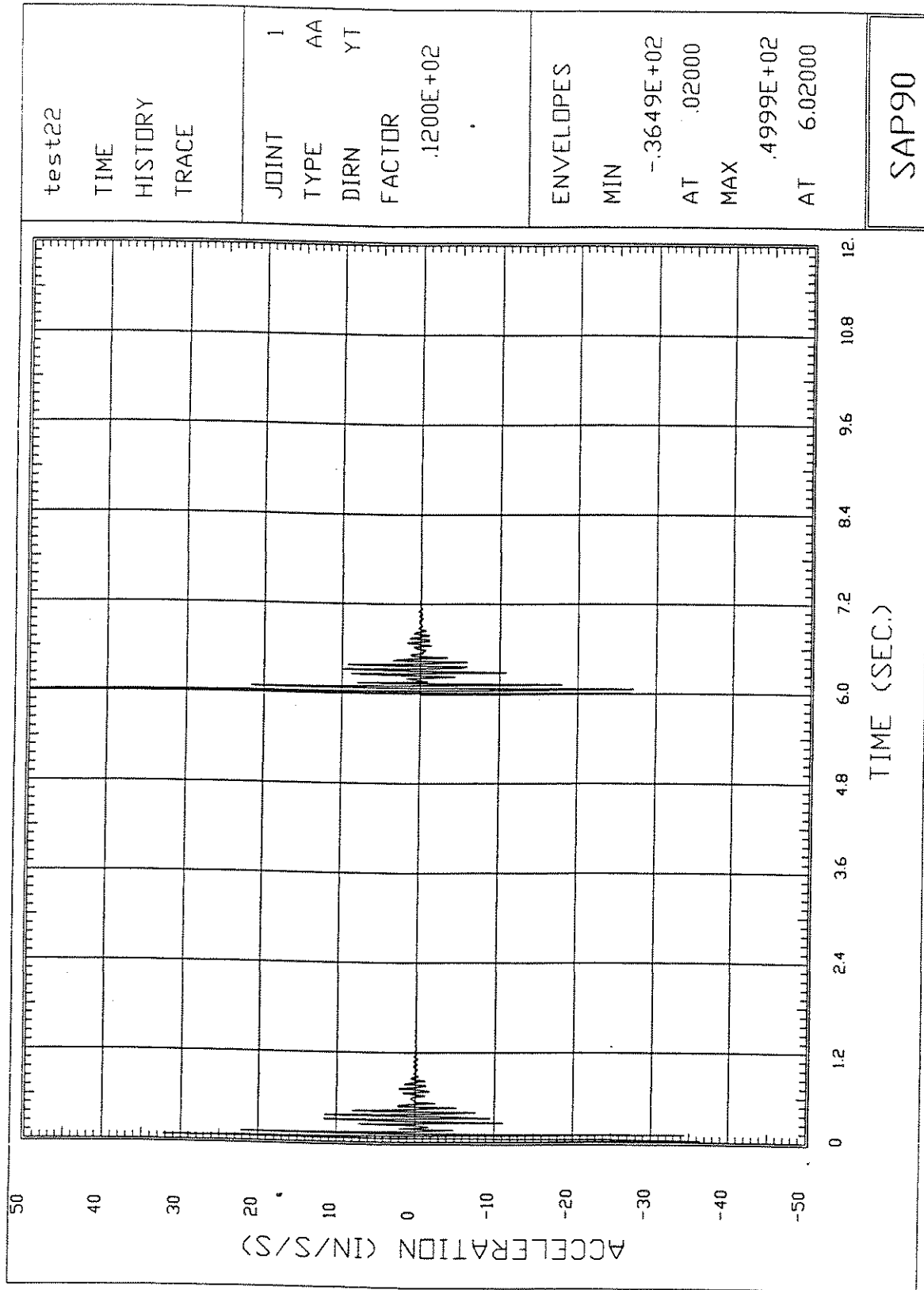


Figure 6.24 Acceleration at Joint 1 in Load Case 3

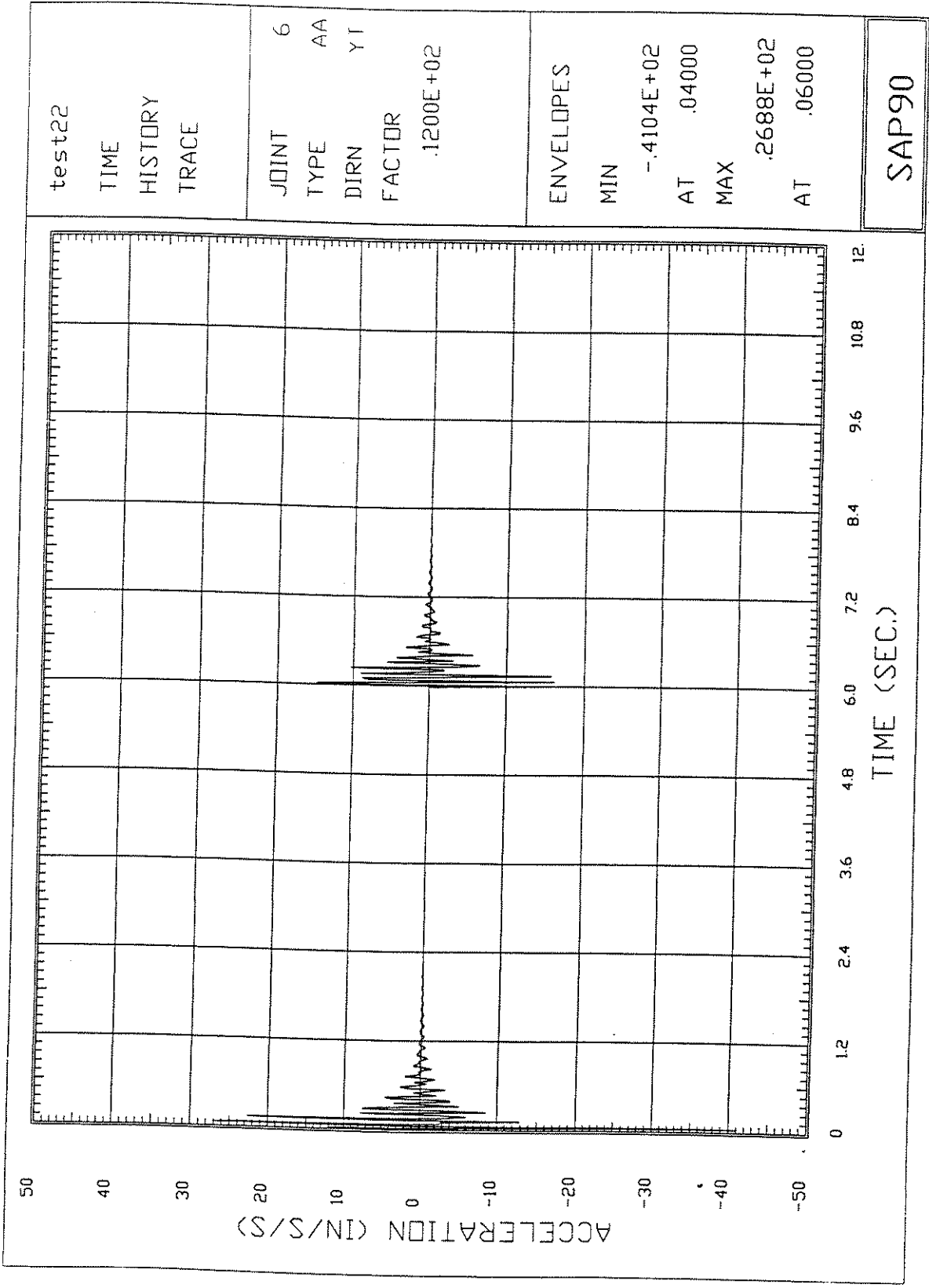


Figure 6.25 Acceleration at Joint 6 in Load Case 3

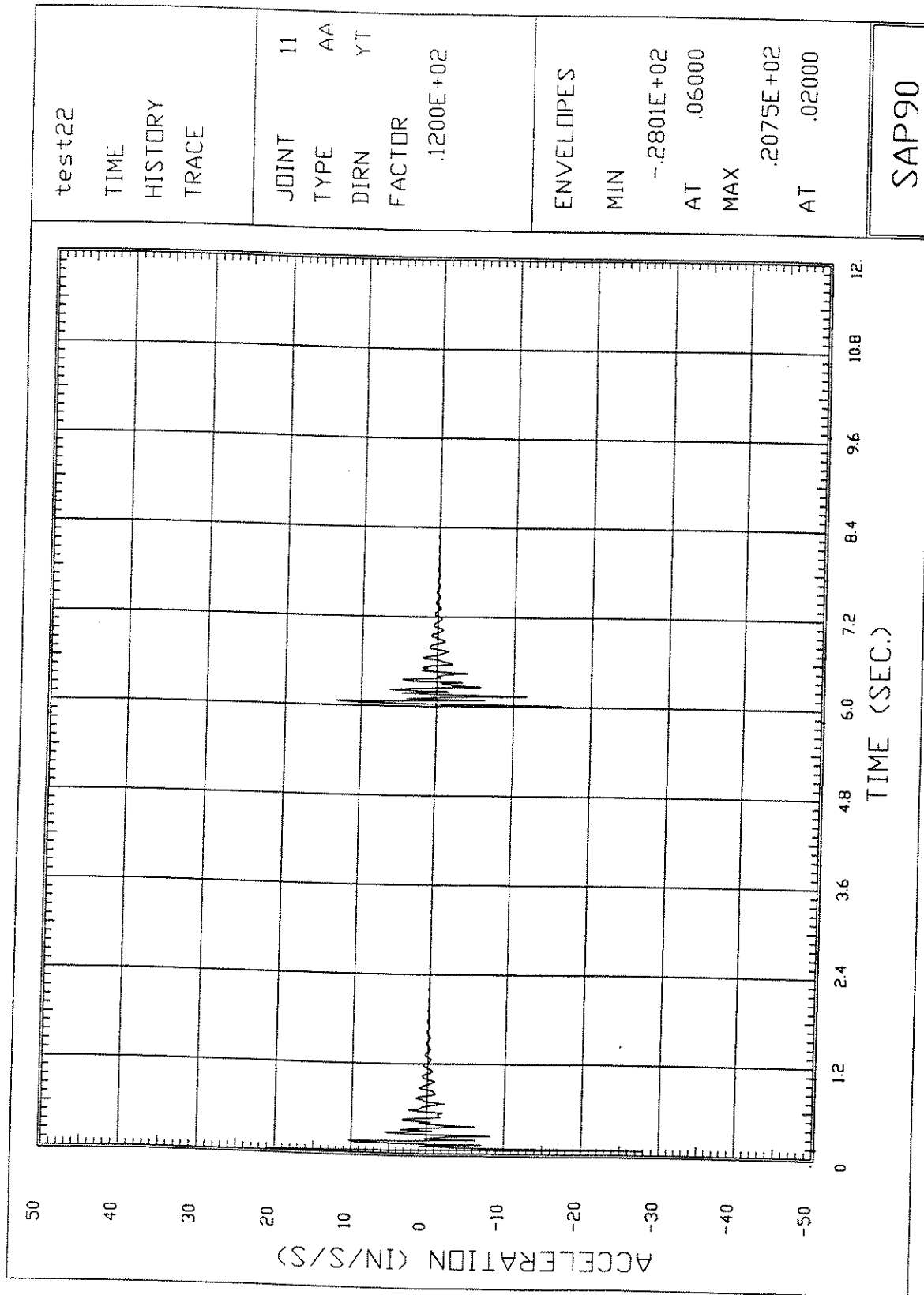


Figure 6.26 Acceleration at Joint 11 in Load Case 3

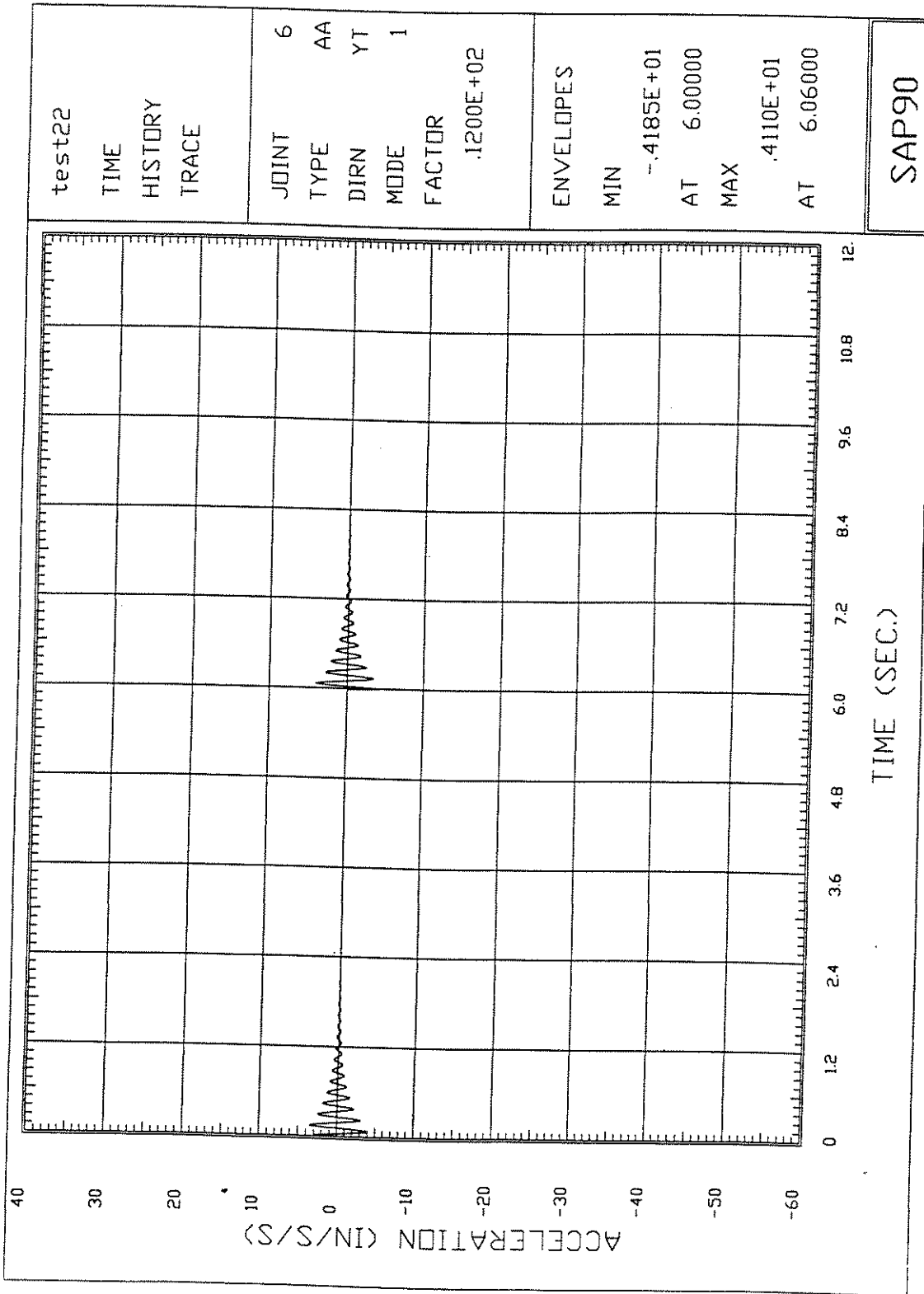


Figure 6.27 Acceleration at Joint 6 (Mode 1) in Load Case 3

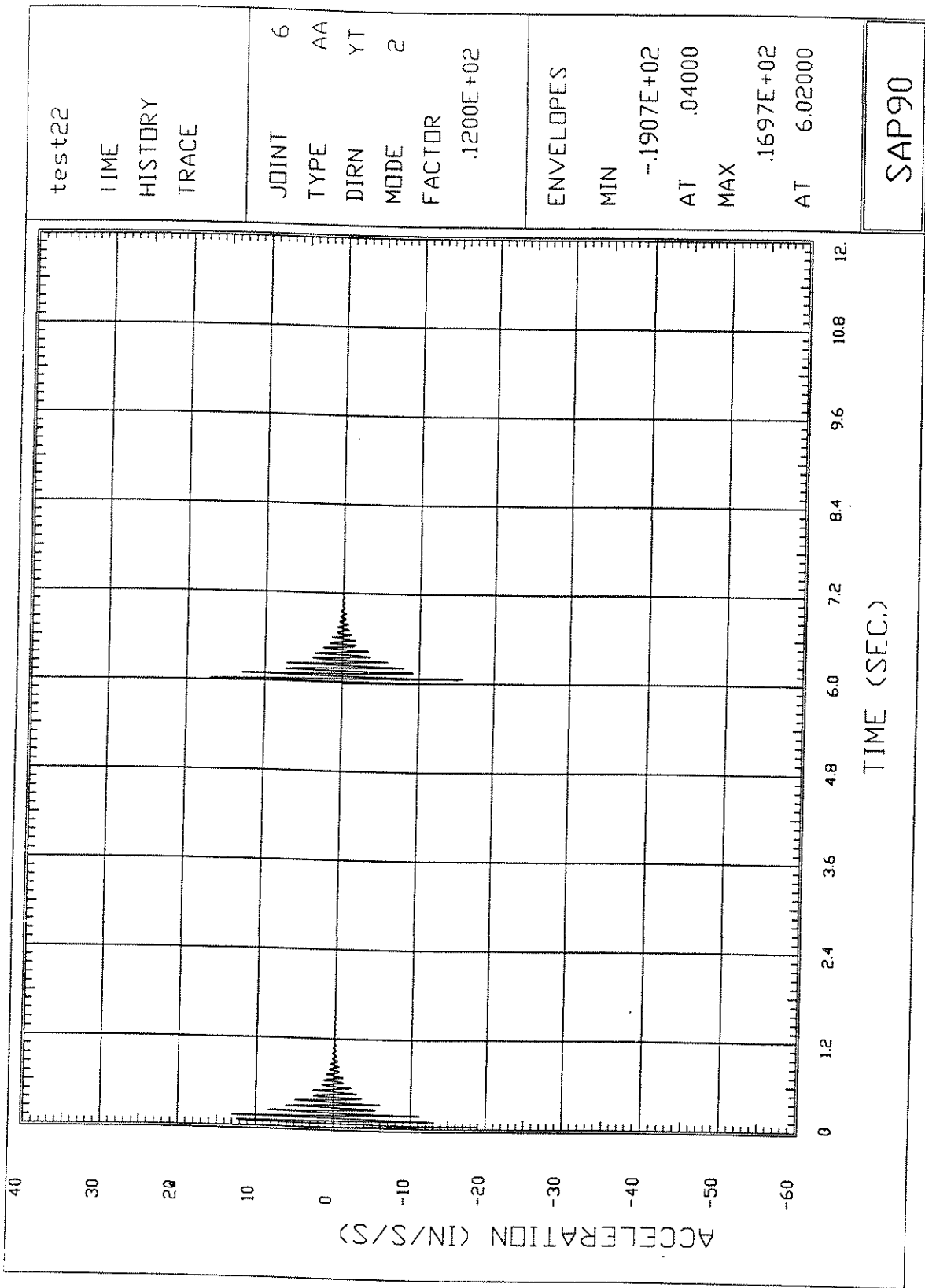


Figure 6.28 Acceleration at Joint 6 (Mode 2) in Load Case 2

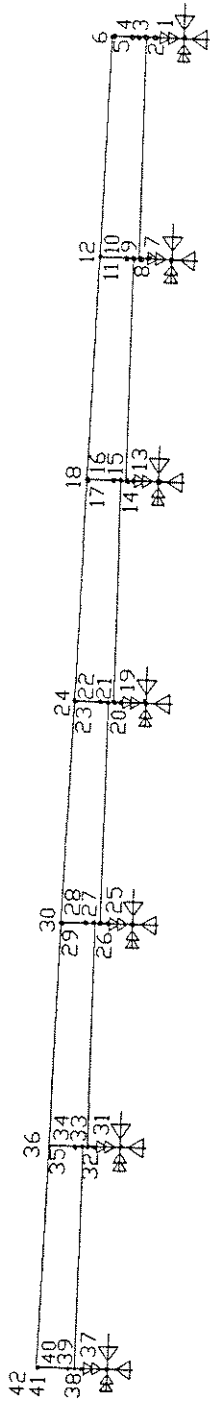


Figure 6.29 Frame-Type Model for Deck and Girder at Pier

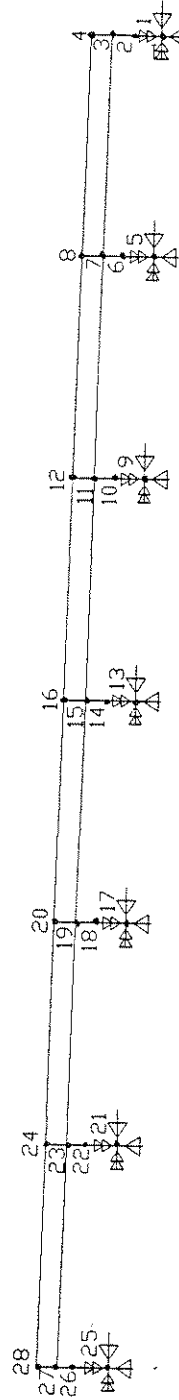


Figure 6.30 Frame-Type Model for Deck and Girder at Abutment

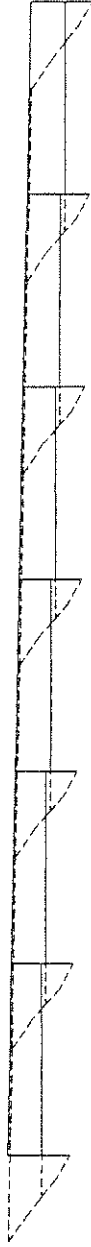


Figure 6.31 Deflection of Frame-Type Model at Pier

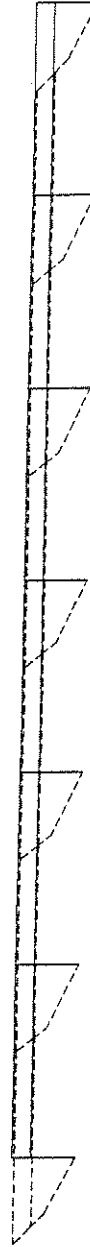


Figure 6.32 Deflection of Frame-Type Model at Abutment

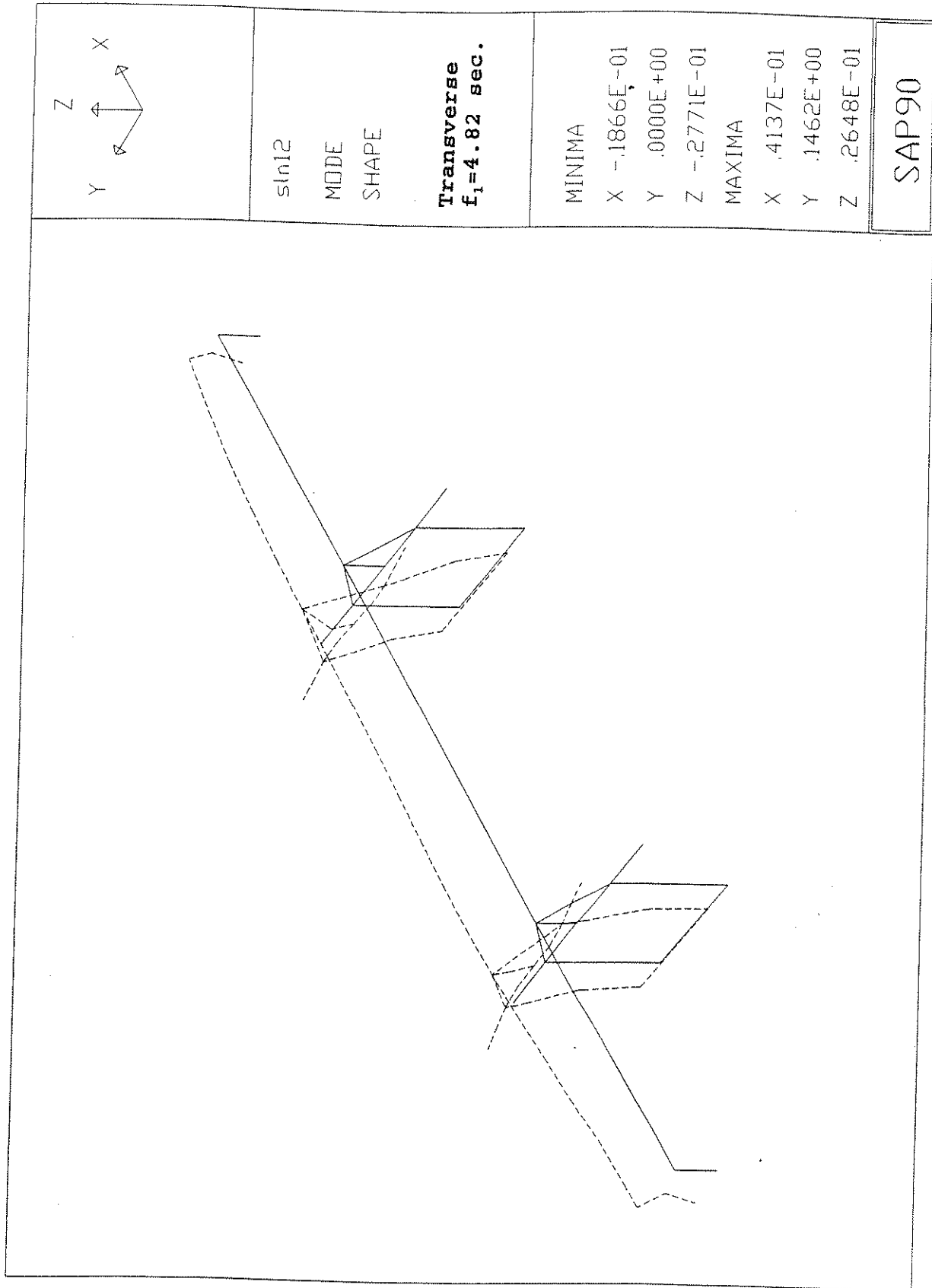


Figure 6.33 The First Transverse Mode Shape of Modified 3-D Model

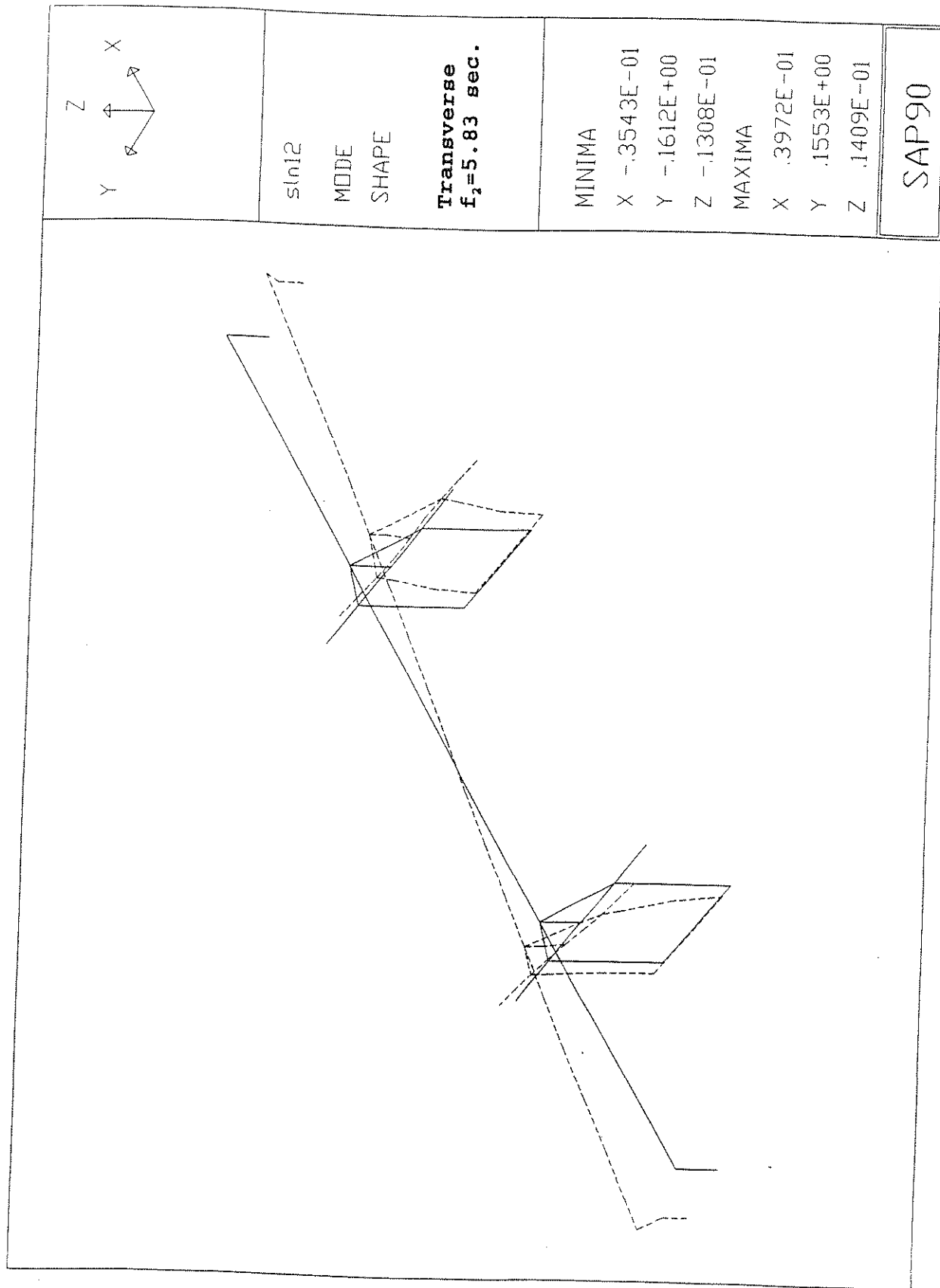
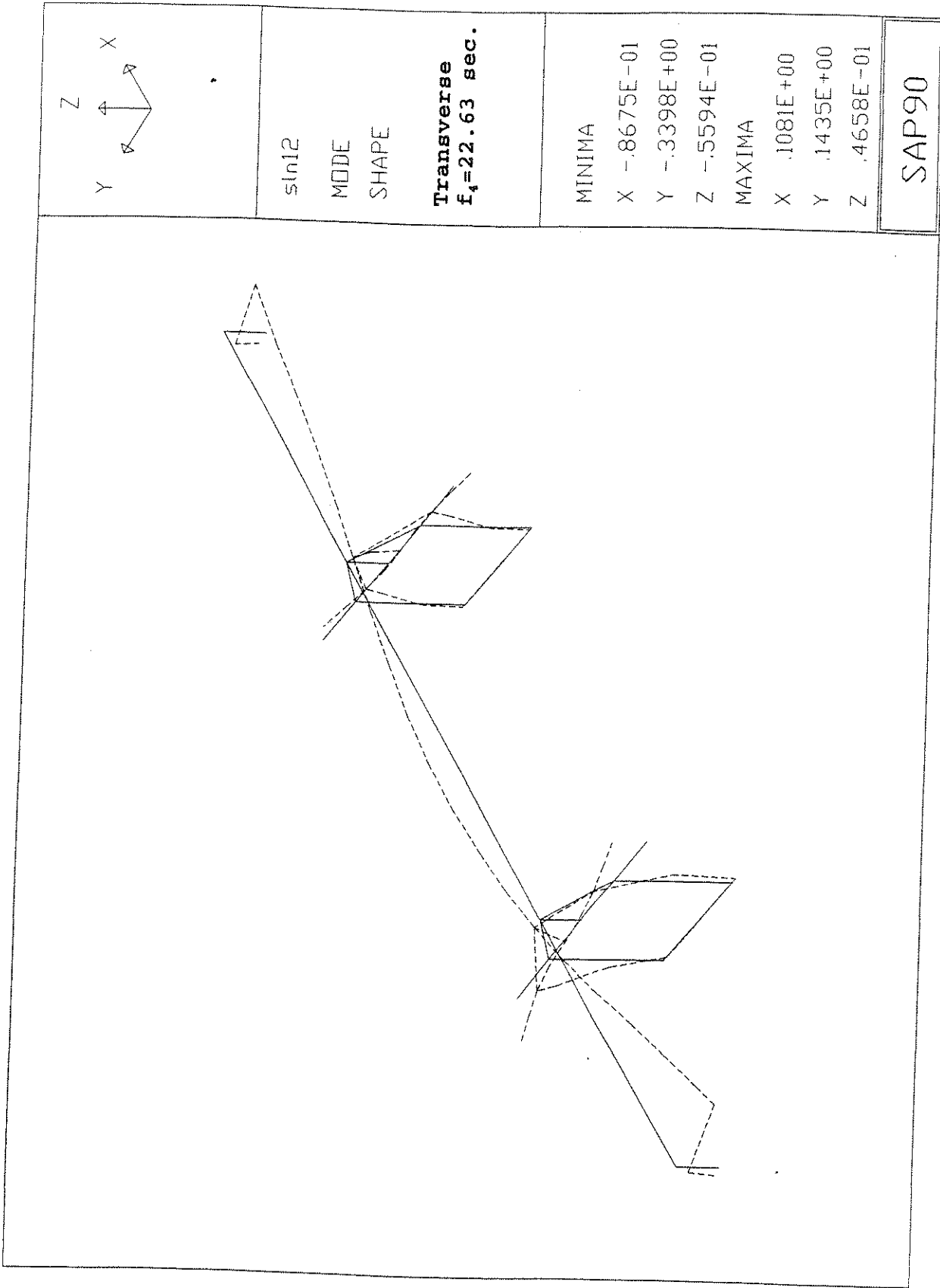


Figure 6.34 The Second Transverse Mode Shape of Modified 3-D Model



sln12
 MODE
 SHAPE

Transverse
 $f_4 = 22.63 \text{ sec.}$

MINIMA

X $-.8675E-01$

Y $-.3398E+00$

Z $-.5594E-01$

MAXIMA

X $.1081E+00$

Y $.1435E+00$

Z $.4658E-01$

SAP90

Figure 6.36 The Fourth Transverse Mode Shape of Modified 3-D Model

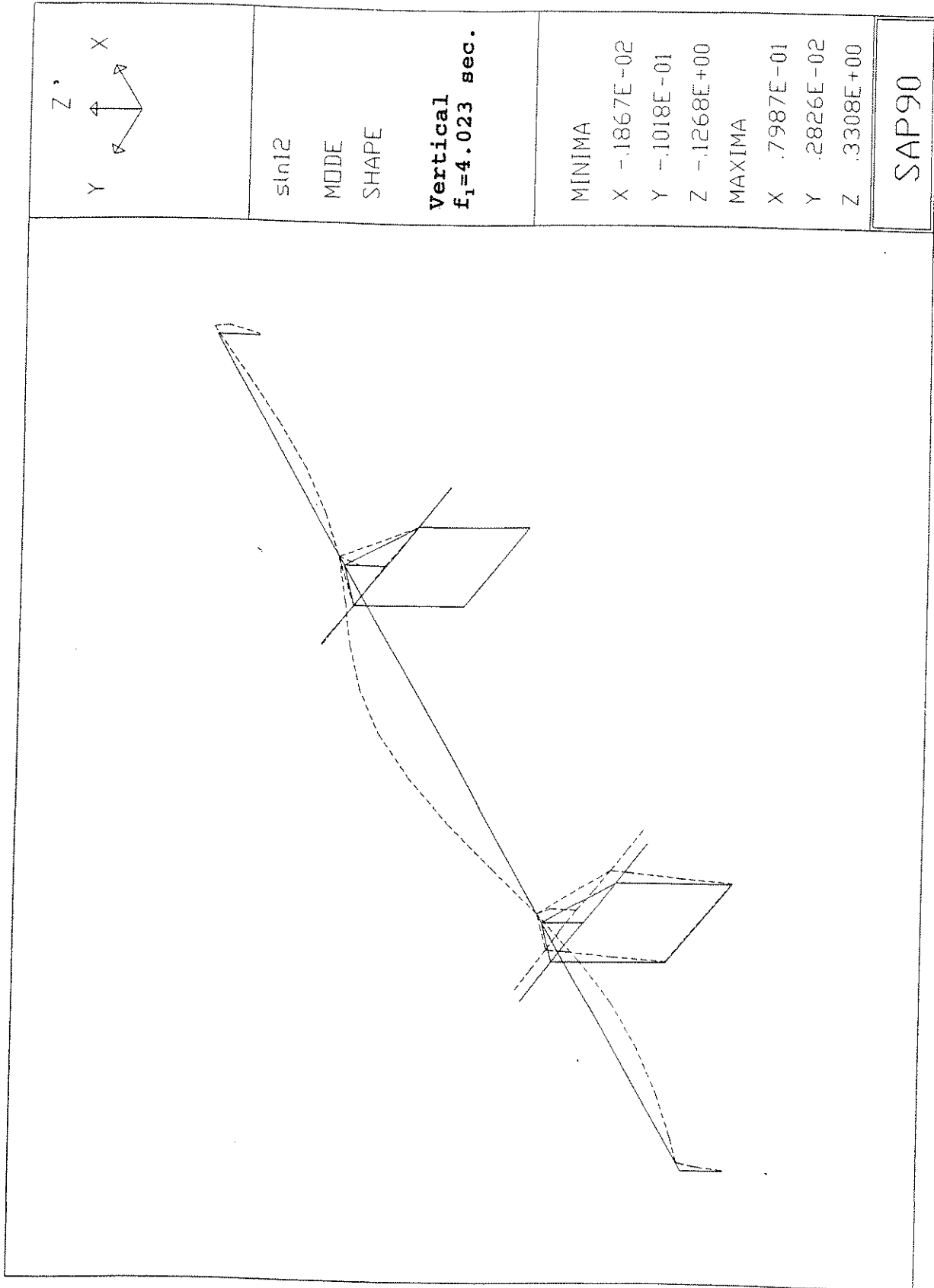
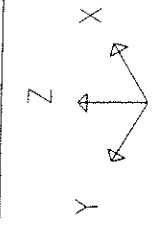
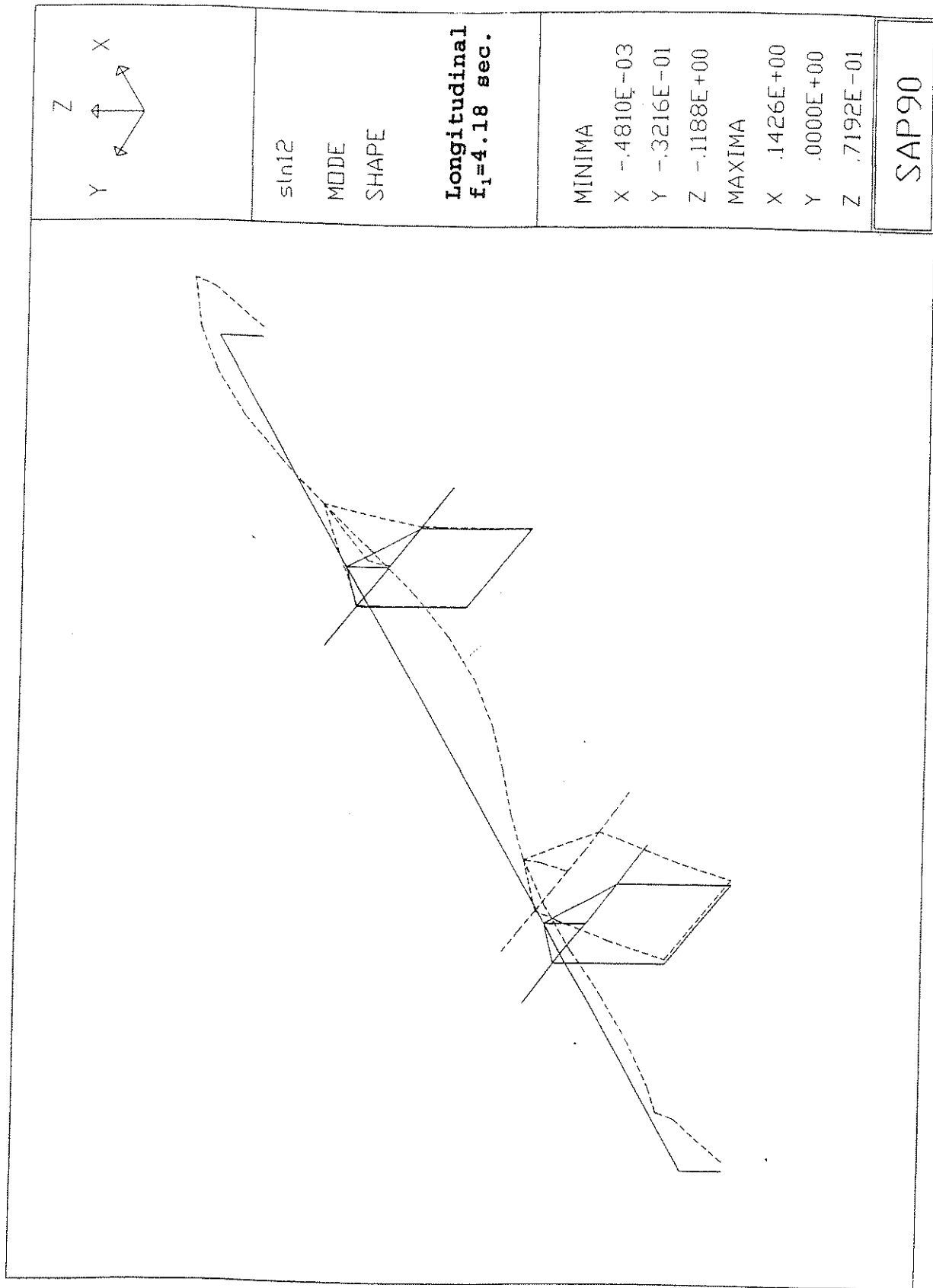


Figure 6.37 The First Vertical Mode Shape of Modified 3-D Model



sln12
 MODE
 SHAPE

Longitudinal
 $f_1=4.18$ sec.

MINIMA

X $-.4810E-03$
 Y $-.3216E-01$
 Z $-.1188E+00$

MAXIMA

X $.1426E+00$
 Y $.0000E+00$
 Z $.7192E-01$

SAP90

Figure 6.38 The First Longitudinal Mode Shape of Modified 3-D Model

List of CCEER Publications

<u>Report No.</u>	<u>Publication</u>
CCEER-84-1	Saiidi, M., and R. A. Lawver. "User's manual for LZAK-C64, a computer program to implement the Q-model on Commodore 64." <i>Report number CCEER-84-1</i> . Reno: University of Nevada, Department of Civil Engineering. January 1984.
CCEER-84-2	Douglas, B. M., and T. Iwasaki. "Proceedings of the first USA-Japan bridge engineering workshop," held at the Public Works Research Institute, Tsukuba, Japan. <i>Report number CCEER-84-2</i> . Reno: University of Nevada, Department of Civil Engineering. April 1984.
CCEER-84-3	Saiidi, M., J. D. Hart, and B. M. Douglas. "Inelastic static and dynamic analysis of short R/C bridges subjected to lateral loads." <i>Report number CCEER-84-3</i> . Reno: University of Nevada, Department of Civil Engineering. July 1984.
CCEER-84-4	Douglas, B. "A proposed plan for a national bridge engineering laboratory." <i>Report number CCEER-84-4</i> . Reno: University of Nevada, Department of Civil Engineering. December 1984.
CCEER-85-1	Norris, G. M., and P. Abdollaholae. "Laterally loaded pile response: Studies with the strain wedge model." <i>Report number CCEER-85-1</i> . Reno: University of Nevada, Department of Civil Engineering. April 1985.
CCEER-86-1	Ghusn, G. E., and M. Saiidi. "A simple hysteretic element for biaxial bending of R/C columns and implementation in NEABS-86." <i>Report number CCEER-86-1</i> . Reno: University of Nevada, Department of Civil Engineering. July 1986.
CCEER-86-2	Saiidi, M., R. A. Lawver, and J. D. Hart. "User's manual of ISADAB and SIBA, computer programs for nonlinear transverse analysis of highway bridges subjected to static and dynamic lateral loads." <i>Report number CCEER-86-2</i> . Reno: University of Nevada, Department of Civil Engineering. September 1986.
CCEER-87-1	Siddharthan, R. "Dynamic effective stress response of surface and embedded footings in sand." <i>Report number CCEER-87-1</i> . Reno: University of Nevada, Department of Civil Engineering. June 1987.
CCEER-87-2	Norris, G., and R. Sack. "Lateral and rotational stiffness of pile groups for seismic analysis of highway bridges." <i>Report number CCEER-87-2</i> . Reno: University of Nevada, Department of Civil Engineering. June 1987.
CCEER-88-1	Orie, J., and M. Saiidi. "A preliminary study of one-way reinforced concrete pier hinges subjected to shear and flexure." <i>Report number CCEER-88-1</i> . Reno: University of Nevada, Department of Civil Engineering. January 1988.
CCEER-88-2	Orie, D., M. Saiidi, and B. Douglas. "A micro-CAD system for seismic design of regular highway bridges." <i>Report number CCEER-88-2</i> . Reno: University of Nevada, Department of Civil Engineering. June 1988.

- CCEER-88-3 Orié, D., and M. Saiidi. "User's manual for Micro-SARB, a microcomputer program for seismic analysis of regular highway bridges." *Report number CCEER-88-3*. Reno: University of Nevada, Department of Civil Engineering. October 1988.
- CCEER-89-1 Douglas, B., M. Saiidi, R. Hayes, and G. Holcomb. "A comprehensive study of the loads and pressures exerted on wall forms by the placement of concrete." *Report number CCEER-89-1*. Reno: University of Nevada, Department of Civil Engineering. February 1989.
- CCEER-89-2a Richardson, J., and B. Douglas. "Dynamic response analysis of the Dominion Road Bridge test data." *Report number CCEER-89-2*. Reno: University of Nevada, Department of Civil Engineering. March 1989.
- CCEER-89-2b Vrontinos, S., M. Saiidi, and B. Douglas. "A simple model to predict the ultimate response of R/C beams with concrete overlays." *Report number CCEER-89-2*. Reno: University of Nevada, Department of Civil Engineering. June 1989.
- CCEER-89-3 Ebrahimpour, A., and P. Jagadish. "Statistical modeling of bridge traffic loads: A case study." *Report number CCEER-89-3*. Reno: University of Nevada, Department of Civil Engineering. December 1989.
- CCEER-89-4 Shields, J., and M. Saiidi. "Direct field measurement of prestress losses in box girder bridges." *Report number CCEER-89-4*. Reno: University of Nevada, Department of Civil Engineering. December 1989.
- CCEER-90-1 Saiidi, M., E. Maragakis, G. Ghush, Jr., Y. Jiang, and D. Schwartz. "Survey and evaluation of Nevada's transportation infrastructure, task 7.2—highway bridges, final report." *Report number CCEER-90-1*. Reno: University of Nevada, Department of Civil Engineering. October 1990.
- CCEER-90-2 Abdel-Ghaffar, S., E. Maragakis, and M. Saiidi. "Analysis of the response of reinforced concrete structures during the Whittier earthquake of 1987." *Report number CCEER-90-2*. Reno: University of Nevada, Department of Civil Engineering. October 1990.
- CCEER-91-1 Saiidi, M., E. Hwang, E. Maragakis, and B. Douglas. "Dynamic testing and analysis of the Flamingo Road Interchange." *Report number CCEER-91-1*. Reno: University of Nevada, Department of Civil Engineering. February 1991.
- CCEER-91-2 Norris, G., R. Siddharthan, Z. Zafir, S. Abdel-Ghaffar, and P. Gowda. "Soil-foundation-structure behavior at the Oakland Outer Harbor Wharf." *Report number CCEER-91-2*. Reno: University of Nevada, Department of Civil Engineering. July 1991.
- CCEER-91-3 Norris, G. M. "Seismic lateral and rotational pile foundation stiffness at Cypress." *Report number CCEER-91-3*. Reno: University of Nevada, Department of Civil Engineering. August 1991.
- CCEER-91-4 O'Connor, D. N., and M. Saiidi. "A study of protective overlays for highway bridge decks in Nevada, with emphasis on polyester-styrene polymer concrete." *Report number CCEER-91-4*. Reno: University of Nevada, Department of Civil Engineering. October 1991.

- CCEER-91-5 O'Connor, D. N., and M. Saiidi. "Laboratory studies of polyester-styrene polymer concrete engineering properties." *Report number CCEER-91-5*. Reno: University of Nevada, Department of Civil Engineering. November 1991.
- CCEER-92-1 Straw, D. L., and M. "Saiid" Saiidi. "Scale model testing of one-way reinforced concrete pier hinges subjected to combined axial force, shear and flexure." *Report number CCEER-92-1*, ed. by D. N. O'Connor. Reno: University of Nevada, Department of Civil Engineering. March 1992.
- CCEER-92-2 Wehbe, N., M. Saiidi, and F. Gordaninejad. "Basic behavior of composite sections made of concrete slabs and graphite epoxy beams." *Report number CCEER-92-2*. Reno: University of Nevada, Department of Civil Engineering. August 1992.
- CCEER-92-3 Saiidi, M., and E. Hutchens. "A study of prestress changes in a post-tensioned bridge during the first 30 months." *Report number CCEER-92-3*. Reno: University of Nevada, Department of Civil Engineering. April 1992.
- CCEER-92-4 Saiidi, M., B. Douglas, S. Feng, E. Hwang, and E. Maragakis. "Effects of axial force on frequency of prestressed concrete bridges." *Report number CCEER-92-4*. Reno: University of Nevada, Department of Civil Engineering. August 1992.
- CCEER-92-5 Siddharthan, R., and Zafir, Z. "Response of layered deposits to traveling surface pressure waves." *Report number CCEER-92-5*. Reno: University of Nevada, Department of Civil Engineering. September 1992.
- CCEER-92-6 Norris, G., and Zafir, Z. "Liquefaction and residual strength of loose sands from drained triaxial tests." *Report number CCEER-92-6*. Reno: University of Nevada, Department of Civil Engineering. September 1992.
- CCEER-92-7 Douglas, B. "Some thoughts regarding the improvement of the University of Nevada, Reno's national academic standing." *Report number CCEER-92-7*. Reno: University of Nevada, Department of Civil Engineering. September 1992.
- CCEER-92-8 Saiidi, M., E. Maragakis, and S. Feng. "An evaluation of the current Caltrans seismic restrainer design method." *Report number CCEER-92-8*. Reno: University of Nevada, Department of Civil Engineering. October 1992.
- CCEER-92-9 O'Connor, D. N., M. Saiidi, and E. A. Maragakis. "Effect of hinge restrainers on the response of the Madrone Drive Undercrossing during the Loma Prieta earthquake." *Report number CCEER-92-9*. Reno: University of Nevada, Department of Civil Engineering. February 1993.
- CCEER-92-10 O'Connor, D. N., and M. Saiidi. "Laboratory studies of polyester concrete: Compressive strength at elevated temperatures and following temperature cycling, bond strength to portland cement concrete, and modulus of elasticity." *Report number CCEER-92-10*. Reno: University of Nevada, Department of Civil Engineering. December 1992.

List of CCEER Publications

<u>Report No.</u>	<u>Publication</u>
CCEER-84-1	Saiidi, M., and R. A. Lawver. "User's manual for LZAK-C64, a computer program to implement the Q-model on Commodore 64." <i>Report number CCEER-84-1</i> . Reno: University of Nevada, Department of Civil Engineering. January 1984.
CCEER-84-2	Douglas, B. M., and T. Iwasaki. "Proceedings of the first USA-Japan bridge engineering workshop," held at the Public Works Research Institute, Tsukuba, Japan. <i>Report number CCEER-84-2</i> . Reno: University of Nevada, Department of Civil Engineering. April 1984.
CCEER-84-3	Saiidi, M., J. D. Hart, and B. M. Douglas. "Inelastic static and dynamic analysis of short R/C bridges subjected to lateral loads." <i>Report number CCEER-84-3</i> . Reno: University of Nevada, Department of Civil Engineering. July 1984.
CCEER-84-4	Douglas, B. "A proposed plan for a national bridge engineering laboratory." <i>Report number CCEER-84-4</i> . Reno: University of Nevada, Department of Civil Engineering. December 1984.
CCEER-85-1	Norris, G. M., and P. Abdollaholhaee. "Laterally loaded pile response: Studies with the strain wedge model." <i>Report number CCEER-85-1</i> . Reno: University of Nevada, Department of Civil Engineering. April 1985.
CCEER-86-1	Ghusn, G. E., and M. Saiidi. "A simple hysteretic element for biaxial bending of R/C columns and implementation in NEABS-86." <i>Report number CCEER-86-1</i> . Reno: University of Nevada, Department of Civil Engineering. July 1986.
CCEER-86-2	Saiidi, M., R. A. Lawver, and J. D. Hart. "User's manual of ISADAB and SIBA, computer programs for nonlinear transverse analysis of highway bridges subjected to static and dynamic lateral loads." <i>Report number CCEER-86-2</i> . Reno: University of Nevada, Department of Civil Engineering. September 1986.
CCEER-87-1	Siddharthan, R. "Dynamic effective stress response of surface and embedded footings in sand." <i>Report number CCEER-87-1</i> . Reno: University of Nevada, Department of Civil Engineering. June 1987.
CCEER-87-2	Norris, G., and R. Sack. "Lateral and rotational stiffness of pile groups for seismic analysis of highway bridges." <i>Report number CCEER-87-2</i> . Reno: University of Nevada, Department of Civil Engineering. June 1987.
CCEER-88-1	Orie, J., and M. Saiidi. "A preliminary study of one-way reinforced concrete pier hinges subjected to shear and flexure." <i>Report number CCEER-88-1</i> . Reno: University of Nevada, Department of Civil Engineering. January 1988.
CCEER-88-2	Orie, D., M. Saiidi, and B. Douglas. "A micro-CAD system for seismic design of regular highway bridges." <i>Report number CCEER-88-2</i> . Reno: University of Nevada, Department of Civil Engineering. June 1988.

- CCEER-88-3 Orie, D., and M. Saiidi. "User's manual for Micro-SARB, a microcomputer program for seismic analysis of regular highway bridges." *Report number CCEER-88-3*. Reno: University of Nevada, Department of Civil Engineering. October 1988.
- CCEER-89-1 Douglas, B., M. Saiidi, R. Hayes, and G. Holcomb. "A comprehensive study of the loads and pressures exerted on wall forms by the placement of concrete." *Report number CCEER-89-1*. Reno: University of Nevada, Department of Civil Engineering. February 1989.
- CCEER-89-2a Richardson, J., and B. Douglas. "Dynamic response analysis of the Dominion Road Bridge test data." *Report number CCEER-89-2*. Reno: University of Nevada, Department of Civil Engineering. March 1989.
- CCEER-89-2b Vrontinos, S., M. Saiidi, and B. Douglas. "A simple model to predict the ultimate response of R/C beams with concrete overlays." *Report number CCEER-89-2*. Reno: University of Nevada, Department of Civil Engineering. June 1989.
- CCEER-89-3 Ebrahimpour, A., and P. Jagadish. "Statistical modeling of bridge traffic loads: A case study." *Report number CCEER-89-3*. Reno: University of Nevada, Department of Civil Engineering. December 1989.
- CCEER-89-4 Shields, J., and M. Saiidi. "Direct field measurement of prestress losses in box girder bridges." *Report number CCEER-89-4*. Reno: University of Nevada, Department of Civil Engineering. December 1989.
- CCEER-90-1 Saiidi, M., E. Maragakis, G. Ghosn, Jr., Y. Jiang, and D. Schwartz. "Survey and evaluation of Nevada's transportation infrastructure, task 7.2—highway bridges, final report." *Report number CCEER-90-1*. Reno: University of Nevada, Department of Civil Engineering. October 1990.
- CCEER-90-2 Abdel-Ghaffar, S., E. Maragakis, and M. Saiidi. "Analysis of the response of reinforced concrete structures during the Whittier earthquake of 1987." *Report number CCEER-90-2*. Reno: University of Nevada, Department of Civil Engineering. October 1990.
- CCEER-91-1 Saiidi, M., E. Hwang, E. Maragakis, and B. Douglas. "Dynamic testing and analysis of the Flamingo Road Interchange." *Report number CCEER-91-1*. Reno: University of Nevada, Department of Civil Engineering. February 1991.
- CCEER-91-2 Norris, G., R. Siddharthan, Z. Zafir, S. Abdel-Ghaffar, and P. Gowda. "Soil-foundation-structure behavior at the Oakland Outer Harbor Wharf." *Report number CCEER-91-2*. Reno: University of Nevada, Department of Civil Engineering. July 1991.
- CCEER-91-3 Norris, G. M. "Seismic lateral and rotational pile foundation stiffness at Cypress." *Report number CCEER-91-3*. Reno: University of Nevada, Department of Civil Engineering. August 1991.
- CCEER-91-4 O'Connor, D. N., and M. Saiidi. "A study of protective overlays for highway bridge decks in Nevada, with emphasis on polyester-styrene polymer concrete." *Report number CCEER-91-4*. Reno: University of Nevada, Department of Civil Engineering. October 1991.

- CCEER-91-5 O'Connor, D. N., and M. Saiidi. "Laboratory studies of polyester-styrene polymer concrete engineering properties." *Report number CCEER-91-5*. Reno: University of Nevada, Department of Civil Engineering. November 1991.
- CCEER-92-1 Straw, D. L., and M. "Saiid" Saiidi. "Scale model testing of one-way reinforced concrete pier hinges subjected to combined axial force, shear and flexure." *Report number CCEER-92-1*, ed. by D. N. O'Connor. Reno: University of Nevada, Department of Civil Engineering. March 1992.
- CCEER-92-2 Wehbe, N., M. Saiidi, and F. Gordaninejad. "Basic behavior of composite sections made of concrete slabs and graphite epoxy beams." *Report number CCEER-92-2*. Reno: University of Nevada, Department of Civil Engineering. August 1992.
- CCEER-92-3 Saiidi, M., and E. Hutchens. "A study of prestress changes in a post-tensioned bridge during the first 30 months." *Report number CCEER-92-3*. Reno: University of Nevada, Department of Civil Engineering. April 1992.
- CCEER-92-4 Saiidi, M., B. Douglas, S. Feng, E. Hwang, and E. Maragakis. "Effects of axial force on frequency of prestressed concrete bridges." *Report number CCEER-92-4*. Reno: University of Nevada, Department of Civil Engineering. August 1992.
- CCEER-92-5 Siddharthan, R., and Zafir, Z. "Response of layered deposits to traveling surface pressure waves." *Report number CCEER-92-5*. Reno: University of Nevada, Department of Civil Engineering. September 1992.
- CCEER-92-6 Norris, G., and Zafir, Z. "Liquefaction and residual strength of loose sands from drained triaxial tests." *Report number CCEER-92-6*. Reno: University of Nevada, Department of Civil Engineering. September 1992.
- CCEER-92-7 Douglas, B. "Some thoughts regarding the improvement of the University of Nevada, Reno's national academic standing." *Report number CCEER-92-7*. Reno: University of Nevada, Department of Civil Engineering. September 1992.
- CCEER-92-8 Saiidi, M., E. Maragakis, and S. Feng. "An evaluation of the current Caltrans seismic restrainer design method." *Report number CCEER-92-8*. Reno: University of Nevada, Department of Civil Engineering. October 1992.
- CCEER-92-9 O'Connor, D. N., M. Saiidi, and E. A. Maragakis. "Effect of hinge restrainers on the response of the Madrone Drive Undercrossing during the Loma Prieta earthquake." *Report number CCEER-92-9*. Reno: University of Nevada, Department of Civil Engineering. February 1993.
- CCEER-92-10 O'Connor, D. N., and M. Saiidi. "Laboratory studies of polyester concrete: Compressive strength at elevated temperatures and following temperature cycling, bond strength to portland cement concrete, and modulus of elasticity." *Report number CCEER-92-10*. Reno: University of Nevada, Department of Civil Engineering. December 1992.